Forschungszentrum Karlsruhe
Technik und Umwelt

Wissenschaftliche Berichte
FZKA 6194

Stellar Neutron Capture Cross Sections of the Yb Isotopes

K. Wisshak, F. Voss, F. Käppeler, L. Kazakov
Institut für Kernphysik

November 1998

FORSCHUNGSZENTRUM KARLSRUHE

Technik und Umwelt

Wissenschaftliche Berichte

FZKA 6194

STELLAR NEUTRON CAPTURE CROSS SECTIONS OF THE Yb ISOTOPES

K. WISSHAK, F. VOSS, F. KÄPPELER, and L. KAZAKOV[1]

Institut für Kernphysik

[1]Institute for Physics and Power Engineering, Obninsk–Kaluga Region, Russia

Forschungszentrum Karlsruhe GmbH, Karlsruhe
1998

Als Manuskript gedruckt

Forschungszentrum Karlsruhe GmbH
Postfach 3640, 76021 Karlsruhe

Mitglied der Hermann von Helmholtz-Gemeinschaft
Deutscher Forschungszentren (HGF)

ISSN 0947-8620

ABSTRACT

The neutron capture cross sections of ^{170}Yb, ^{171}Yb, ^{172}Yb, ^{173}Yb, ^{174}Yb, and ^{176}Yb have been measured in the energy range from 3 to 225 keV at the Karlsruhe 3.75 MV Van de Graaff accelerator. Neutrons were produced via the ^{7}Li$(p,n)^{7}$Be reaction by bombarding metallic Li targets with a pulsed proton beam. Capture events were registered with the Karlsruhe 4π Barium Fluoride Detector. The cross sections were determined relative to the gold standard. Neutron capture in the even ytterbium isotopes is characterized by a strong population of isomeric states, resulting in severe systematic uncertainties in previous experiments. In the present work, the partial cross sections to the ground- and isomeric states in ^{172}Yb, ^{174}Yb, ^{176}Yb could be experimentally separated for the first time, yielding cross section ratios with an overall uncertainty of 1–1.5%. Compared to previous measurements, this corresponds to an improvement by factors of 4 to 10.

Maxwellian averaged neutron capture cross sections were calculated for thermal energies between kT = 8 keV and 100 keV. The results of four isotopes differ by more than 15% from recent evaluations.

ZUSAMMENFASSUNG

DIE STELLAREN (n,γ) QUERSCHNITTE DER Yb ISOTOPE

Die Neutroneneinfangquerschnitte von ^{170}Yb, ^{171}Yb, ^{172}Yb, ^{173}Yb, ^{174}Yb und ^{176}Yb wurden im Energiebereich von 3 bis 225 keV am Karlsruher Van de Graaff Beschleuniger relativ zu Gold als Standard bestimmt. Neutronen wurden über die ^{7}Li(p,n)^{7}Be–Reaktion durch Beschuß metallischer Li–Targets mit einem gepulsten Protonenstrahl erzeugt, und Einfangereignisse wurden mit dem Karlsruher 4π Barium Fluorid Detektor nachgewiesen. Die Querschnitte wurden relativ zum (n,γ)–Querschnitt von Gold als Standard bestimmt. Neutroneneinfang in den geraden Ytterbiumisotopen ist durch eine starke Bevölkerung von isomeren Zuständen gekennzeichnet, die in früheren Experimenten zu starken systematischen Unsicherheiten führte. In dieser Arbeit konnten die Partialquerschnitte zu Grundzustand und Isomer in ^{172}Yb, ^{174}Yb, ^{176}Yb erstmals experimentell getrennt werden. Die so bestimmten Querschnittsverhältnisse sind mit einer Unsicherheit von 1–1.5% um Faktoren 4 bis 10 genauer als frühere Ergebnisse.

Die stellaren Einfangquerschnitte wurden für thermische Energien von kT = 8 keV bis 100 keV berechnet. Für vier der untersuchten Isotope weichen die Ergebnisse um mehr als 15% von den evaluierten Datensätzen ab.

Contents

1 INTRODUCTION

The present measurement of the (n,γ) cross sections of the ytterbium isotopes is part of a comprehensive study of the rare earth region with the Karlsruhe $4\pi BaF_2$ detector [1, 2, 3, 4]. This project is motivated by the need for an accurate data basis to study the nucleosynthesis of the heavy elements in the slow neutron capture process (s process). The rare earth region is of special importance in this respect since the solar abundances of these chemically almost identical elements are much better defined than those of the other elements [5]. Hence, the characteristic s-process feature, the product of s–process abundance and stellar capture cross section, $N_s\langle\sigma\rangle$, can be reliably determined in this particular mass region between ^{139}La and ^{176}Lu.

The s–process path around ytterbium is sketched in Fig. 1. The s–only isotope ^{170}Yb is shielded by its stable Er isobar from contributions from the r process. Its abundance provides a measure for the strength of the weak branchings at ^{169}Er and ^{170}Tm. A recent study in the framework of the classical model [6] showed, that ^{170}Yb may be significantly overproduced. This implies, that either the branching is much stronger than expected, that the cross sections used are in error, or that the model is inadequate to describe this region of the s-process path.

The s-process contribution to the rare earth isotopes is produced during helium shell burning in low mass stars. This asymptotic giant branch (AGB) phase is characterized by successive thermal instabilities where neutrons are released in two different ways [7]. A long pulse of low neutron density is produced under radiative conditions between subsequent thermal instabilities via the $^{12}C(\alpha,n)$ reaction, followed by a short burst with high neutron density during the next thermal instability when the $^{22}Ne(\alpha,n)$ reaction is ignited in the convectively burning He shell.

In a recent paper by Gallino *et al.* [8], ^{170}Yb is explicitely mentioned as a suited test case for studying the freeze-out of the neutron flux. Due to its high cross section ^{170}Yb is depleted in the second neutron burst by more than one order of magnitude, and freeze-out of the abundance pattern of that branching (i.e.the final ^{170}Yb abundance) is reached at a neutron density of $\sim 6\times10^7$n/s. The effective thermal energy during this pulse being kT=23 keV demonstrates that the physical parameters in the stellar model are significantly different from those of the steady solution of the classical approach, from which a neutron density of 4.1×10^8n/s and a thermal energy of 29 keV are deduced.

From a previous measurement of the ytterbium cross sections, two sets of data have been published [9, 10], which exhibit reasonable agreement for most of the isotopes, but differ by 30% in case of the small cross section of ^{176}Yb. The important cross section of the s-only isotope ^{170}Yb has also been measured twice by Beer et al. [11, 12]. Also these results agree reasonably well, and are supported by the results of Allen and Cohen [13]. However, these data are almost 40% lower than the first two data sets. A rather old measurement on ^{176}Yb [14] reported a roughly two times larger cross section than has

been measured later.

Neutron capture on the even ytterbium isotopes is known to significantly populate a number of long-lived isomers. In cross section measurements with conventional techniques based on Moxon-Rae detectors or on total energy detectors with pulse height weighting, this feature results in an inherent uncertainty. In such experiments, the sum energy of the capture cascade – represented by the binding energy of the captured neutron (increased by its small kinetic energy) – is directly used in data evaluation as a fixed parameter. Since these techniques do not allow to distinguish capture cascades feeding the ground state or the isomer, events leading to the isomer are evaluated with too high binding energies. This effect may well cause systematic uncertainties of the order of 10%.

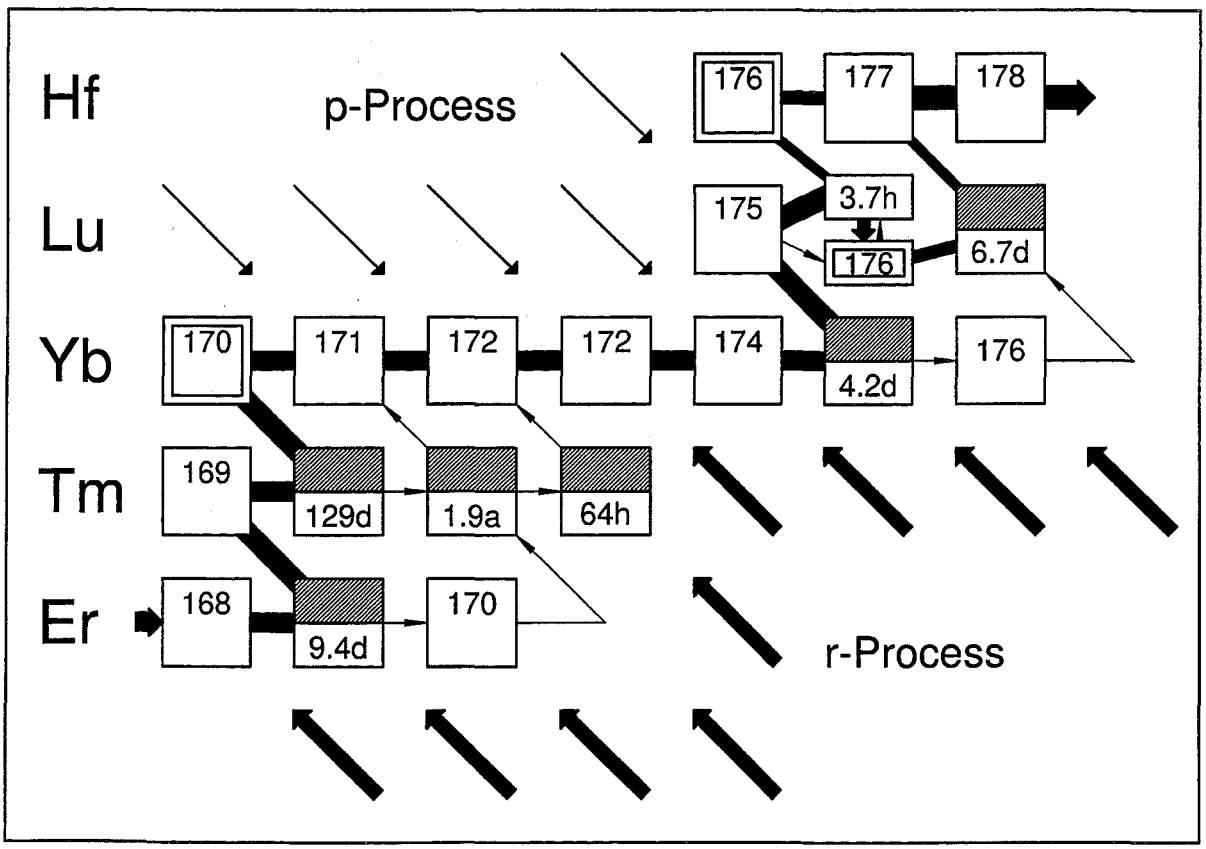

Figure 1: The reaction path of the s process in the region of the ytterbium isotopes.

Since systematic uncertainties related to the population of isomeric states can be avoided in the present experiment, it is intended to resolve the existing discrepancies in the stellar (n,γ) cross sections of the ytterbium isotopes and to establish a reliable basis for a detailed s-process analysis of the branchings at A=169/170.

Measurements and data analysis are described in Secs. 2 and 3, followed by a discussion of the results and uncertainties in Secs. 4 and 5. The stellar cross sections are presented in Sec. 6. The astrophysical implications will be addressed in a forthcoming publication.

2 EXPERIMENT

The neutron capture cross sections of the ytterbium isotopes 170 to 174 and 176 have been measured in the energy range from 3 to 225 keV using gold as a standard. Since the experimental method has been published in detail [1, 15, 16, 17], only a general description is given here, complemented with the specific features of the present measurement.

Neutrons were produced via the ^{7}Li$(p,n)^7$Be reaction by bombarding metallic Li targets with the pulsed proton beam of the Karlsruhe 3.75 MV Van de Graaff accelerator. The neutron energy was determined by time of flight (TOF), the samples being located at a flight path of 79 cm. The relevant parameters of the accelerator were a pulse width of <1 ns, a repetition rate of 250 kHz, and an average beam current of 2.2 μA. In different runs, the proton energies were adjusted 30 and 100 keV above the threshold of the ^{7}Li$(p,n)^7$Be reaction at 1.881 MeV. In this way, continuous neutron spectra in the proper energy range for s–process studies were obtained, ranging from 3 to 100 keV, and 3 to 225 keV, respectively. The lower maximum neutron energy offers a significantly better signal-to-background ratio at lower energies.

Capture events were registered with the Karlsruhe 4π Barium Fluoride Detector via the prompt capture γ–ray cascades. This detector consists of 42 hexagonal and pentagonal crystals forming a spherical shell of BaF_2 with 10 cm inner radius and 15 cm thickness. It is characterized by a resolution in γ–ray energy of 7% at 2.5 MeV, a time resolution of 500 ps, and a peak efficiency of 90% at 1 MeV. The 1.6 MeV threshold in γ–ray energy used in the present experiment corresponds to an efficiency for capture events of more than 95% for all investigated isotopes. A comprehensive description of this detector can be found in Ref. [16].

The experiment was divided into three runs, two using the conventional data acquisition technique with the detector operated as a calorimeter, and one with an ADC system coupled to the detector for analyzing the signals from all modules individually. In this way, the full spectroscopic information recorded by the detector can be recovered.

The ytterbium samples were prepared from isotopically enriched oxide powder (Yb_2O_3) which was heated to 1200 K for 15 min to eliminate any water contaminations. Then the various batches were pulverized in an agate mortar, pressed into pellets of 15 mm diameter, and reheated to 1200 K for 1 hour. During the final heating the pellets shrank slightly. Immediately after cooling, the actual samples were prepared by canning the pellets into air tight aluminum cylinders with 0.2 mm thick walls. In the first heating step the various batches of enriched isotopes lost between 0.3% and 1.0% in weight, whereas no further losses could be observed in the second step.

In addition to the 6 ytterbium samples, a gold sample in an identical Al can was used for measuring the neutron flux. An empty can was mounted on the sample ladder for determining the sample independent background, and a graphite sample served for simulating the background due to scattered neutrons. The relevant sample parameters are compiled in Table 1, and the isotopic composition of the ytterbium samples provided by the supplier (IPPE Obninsk) is listed in Table 2.

The neutron transmission of the samples calculated with the SESH code [18] was generally larger than 90% (Table 3). The measured spectra of all samples were normalized to equal neutron flux by means of a ^{6}Li–glass monitor located close to the neutron target.

The transmission spectra measured with a second ^{6}Li–glass detector at a flight path of 260 cm were used for a rough determination of the total cross sections. Though the accuracy of this method is inferior to that obtained in a dedicated experiment, these total cross sections can be used in the calculation of the multiple scattering correction.

The samples were moved cyclically into the measuring position by a computer controlled sample changer. The data acquisition time per sample was about 10 min, a complete cycle lasting about 1.3 h. From each event, a 64 bit word was recorded on DAT tape containing the sum energy and TOF information together with 42 bits identifying those detector modules that contributed. The relevant parameters of the three runs corresponding to neutron spectra with different maximum energies are listed in Table 4. The data in Run III were recorded with the ADC system.

Table 1: SAMPLE CHARACTERISTICS

Sample	Diameter	Thickness		Weight[a]	Can[b]	Neutron binding
	(mm)	(mm)	(10^{-3}at/barn)[c]	(g)	(g)	energy (MeV)
^{174}Yb	14.8	4.7	7.8174	4.5420	0.3403	5.822
Graphite	15.0	2.5	21.708	0.7651	0.3058	
^{171}Yb	14.7	0.9	1.5541	0.8899	0.2526	8.020
^{170}Yb	14.8	2.4	3.9842	2.2749	0.2757	6.614
^{197}Au	15.0	0.4	2.2483	1.2995	0.2662	6.513
^{172}Yb	14.7	3.3	4.9429	2.8439	0.2802	6.367
^{173}Yb	14.9	1.8	2.5375	1.4674	0.2826	7.465
Empty	15.0				0.2422	
^{176}Yb	14.8	4.7	7.7144	4.5243	0.3231	5.567

[a]For ytterbium samples: weight of Yb_2O_3
[b]Aluminum cylinder
[c]For ytterbium samples: sum of all Yb isotopes

Table 2: ISOTOPIC COMPOSITION (%)

Sample	Isotope					
	^{170}Yb	^{171}Yb	^{172}Yb	^{173}Yb	^{174}Yb	^{176}Yb
^{170}Yb	70.42	13.26	9.10	3.33	3.17	0.72
^{171}Yb	0.69	89.10	7.16	1.53	1.37	0.15
^{172}Yb	0.00	0.50	94.10	3.60	1.60	0.20
^{173}Yb	0.03	0.23	2.51	87.60	9.28	0.35
^{174}Yb	0.04	0.16	0.30	0.60	98.10	0.80
^{176}Yb	0.10	0.53	0.87	0.73	2.47	95.30

Table 3: CALCULATED NEUTRON TRANSMISSION[a]

Sample	Neutron Energy (keV)				
	10	20	40	80	160
^{197}Au	0.959	0.965	0.970	0.974	0.979
^{170}Yb	0.921	0.930	0.937	0.943	0.949
^{171}Yb	0.971	0.974	0.976	0.978	0.980
^{172}Yb	0.913	0.920	0.926	0.932	0.937
^{173}Yb	0.952	0.957	0.961	0.964	0.967
^{174}Yb	0.868	0.875	0.883	0.891	0.900
^{176}Yb	0.873	0.881	0.890	0.898	0.906

[a] Monte Carlo calculation with SESH code [18].

Table 4: PARAMETERS OF THE INDIVIDUAL RUNS

Run	Flight Path (mm)	TOF Scale (ns/ch)	Number of Cycles	Maximum Neutron Energy (keV)	Measuring Time (d)	Mode of Operation	Average Beam Current (μA)	Threshold in Sum Energy (MeV)
I	788.1	0.7600	259	100	19.0	Calorimeter	1.7	1.75
II	788.0	0.7601	235	200	11.7	Calorimeter	2.4	1.60
III	787.8	0.7091	269	100	13.6	ADC	2.4	1.60

3 DATA ANALYSIS

3.1 Total Cross Sections

The total cross sections of the investigated isotopes were determined in the neutron energy range from 10 to 200 keV via the TOF spectra measured with the ^{6}Li glass detector at a flight path of 260 cm. The total cross sections and the related uncertainties were obtained as described in Ref. [1], and are listed in Table 5. The results deduced for the carbon sample agree with the data from the Joint Evaluated File (JEF) [19] within $\pm$2.0%. The quoted uncertainties were obtained under the assumption that they are inversely proportional to the fraction of neutrons interacting in the sample, A=1–T, where T is the transmission. For the carbon sample this fraction is A=9.2%, the related uncertainty of 2.0% being estimated from the comparison with the JEF data. The oxygen cross section was adopted from the JEF evaluation and its uncertainty was neglected. According to the above relation, the uncertainty was entirely ascribed to the respective ytterbium isotope. The cross section for elemental ytterbium, which was calculated from the isotopic contributions but neglecting the rare isotope ^{168}Yb, was found in good agreement with the data given in Ref. [20].

Table 5: MEASURED TOTAL CROSS SECTIONS [a]

Neutron Energy	Total Cross Section (barn)							
(keV)	^{170}Yb	^{171}Yb	^{172}Yb	^{173}Yb	^{174}Yb	^{176}Yb	^{12}C	^{197}Au
10 – 15	15.3	11.1	9.6	12.5	9.8	11.1	4.49	13.0
15 – 20	14.5	11.9	11.8	11.7	10.6	11.0	4.70	14.3
20 – 30	12.9	10.9	10.8	10.7	12.4	9.9	4.54	12.9
30 – 40	12.6	10.2	10.5	9.7	11.5	10.3	4.47	12.8
40 – 60	11.2	10.9	10.5	9.9	10.6	8.8	4.50	12.0
60 – 80	10.9	9.7	9.4	8.6	8.8	8.2	4.42	11.6
80 – 100	10.0	9.1	8.6	8.5	8.6	7.9	4.23	10.7
100 – 150	9.0	8.6	8.0	8.4	8.2	7.8	4.12	9.6
150 – 200	9.1	9.2	8.2	9.7	8.0	8.1	4.14	8.7
Typical Uncertainty (%)	4.0	10.4	3.7	7.3	2.3	2.7	2.0	6.6

[a]Determined from the count rate of the ^{6}Li glass neutron monitor at 260 cm flight path

3.2 Capture Cross Sections

The analysis was carried out in the same way as described previously [1, 15, 17]. All events were sorted into two–dimensional spectra containing 128 sum energy versus 2048 TOF channels according to various event multiplicities (Evaluation 1). In Evaluation 2, this procedure was repeated by rejecting those events, where only neighboring detector modules contributed to the sum energy signal. With this option, background from the natural radioactivity of the BaF_2 crystals and from scattered neutrons can be reduced. For all samples, the resulting spectra were normalized to equal neutron flux using the count rate of the ^{6}Li glass monitor close to the neutron target. The corresponding normalization factors are below 0.5% for all runs. The treatment of the two–dimensional spectra from the data recorded with the ADC system is slightly more complicated and was performed as described in Ref. [1].

In the next step of data analysis, sample–independent backgrounds were removed by subtracting spectra measured with the empty can. A remaining constant background was determined at very long flight times, where no time–correlated events are expected. The resulting two–dimensional spectra for events with multiplicity >2 measured in Run III are shown for all investigated isotopes in Figs. 2, 3, and 4. Note that events with low sum–energy and large TOF are suppressed by a preprocessing option of the ADC–system.

At this point, the spectra contain only events correlated with the sample. The next correction to be made is for isotopic impurities (see Ref.[1] for details). The respective coefficients are compiled in Table 6.

In Fig. 5 the TOF spectra of the ^{170}Yb sample before subtraction of the background from isotopic impurities are shown together with this background. The correction is about 18% of the measured effect. For all other samples it is below 8%.

As discussed in Ref. [2] the present method to correct for isotopic impurities holds exactly only if all samples are about equal in weight: only then second order effects due

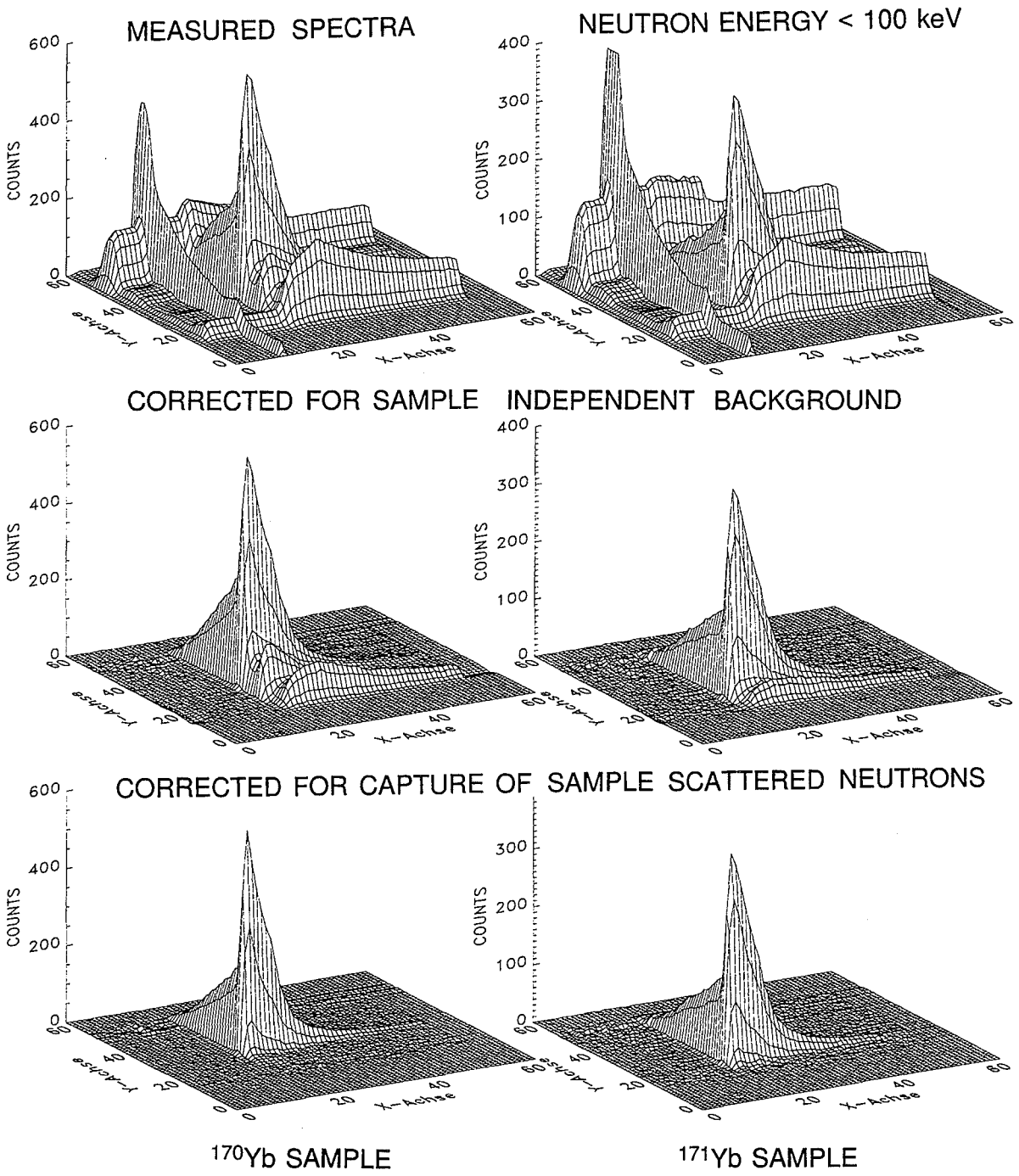

Figure 2: The different steps of background subtraction in the two-dimensional sum energy × TOF spectra. The data are shown for ^{170}Yb and ^{171}Yb measured in Run III with 100 keV maximum neutron energy and an event multiplicity >2. (The original resolution of 128 × 2048 channels was compressed into 64 × 64 channels for better readability. The TOF is plotted on the X–axis and the sum–energy on the Y–axis).

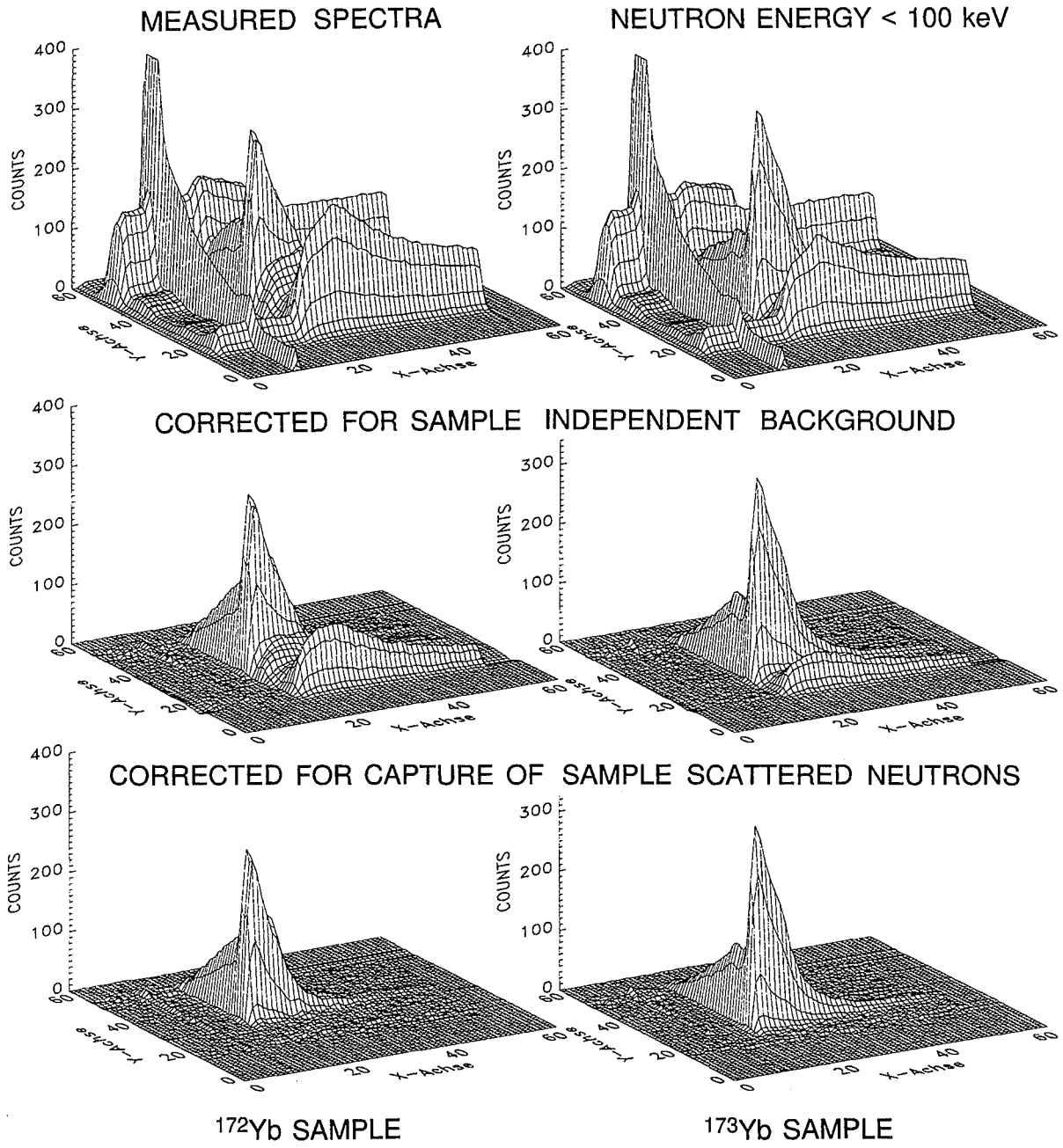

Figure 3: As Fig. 2 but for the ^{172}Yb and ^{173}Yb samples.

to neutron multiple scattering and self–absorption are properly accounted for. In the present experiment the largest correction occurs for the ^{170}Yb sample due to the ^{171}Yb admixture of 13.3%. The weight of the two samples differs by a factor of 2.6. Therefore, calculating the correction directly from the isotopic matrix leads to an overcompensation due to the smaller self–shielding effect in the thin ^{171}Yb sample. With the good energy resolution of the $4\pi BaF_2$ detector, this effect can be verified in the corrected sum energy spectrum of ^{170}Yb where a negative peak is obtained at the binding energy of ^{171}Yb. The

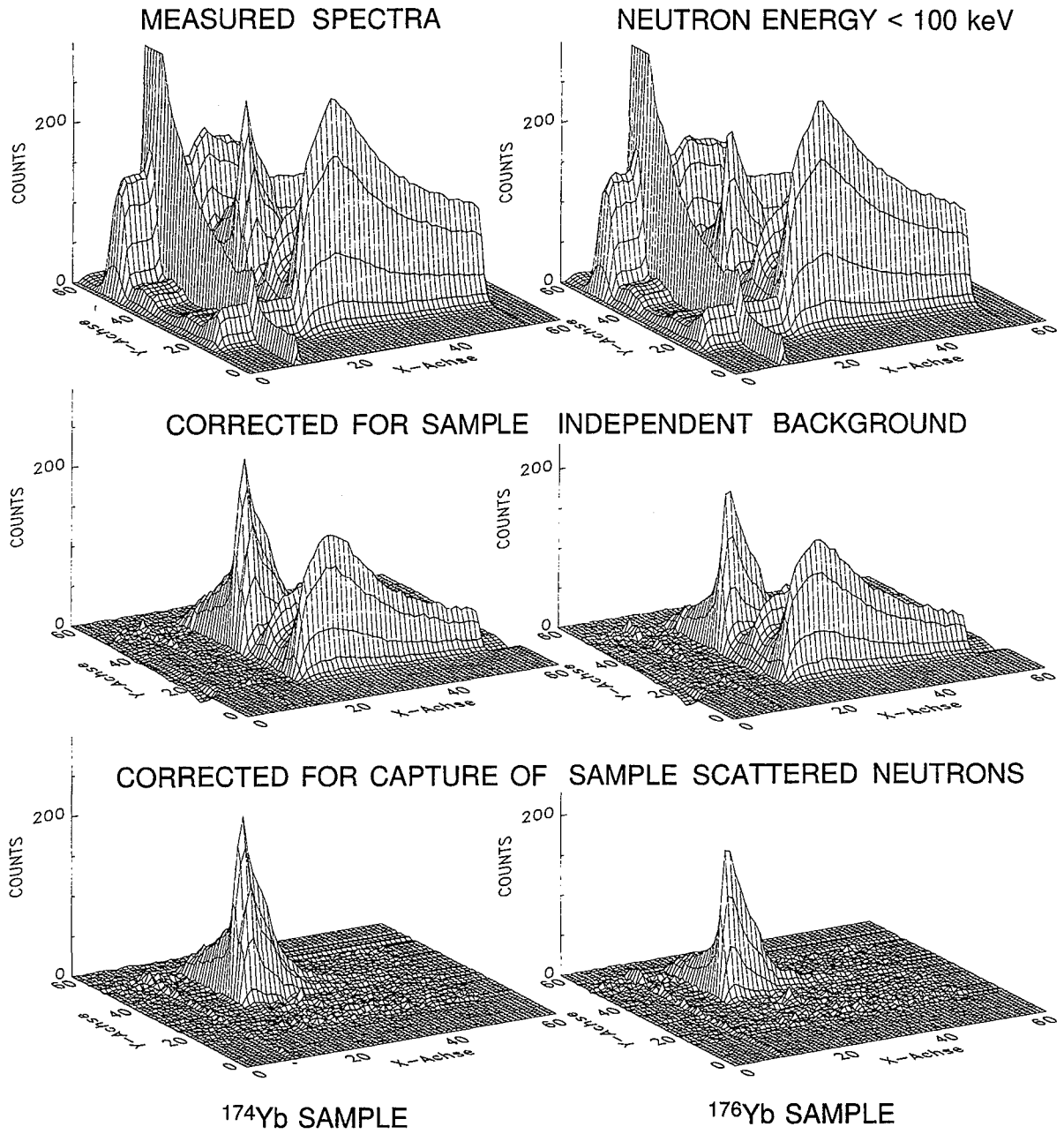

Figure 4: As Fig. 2 but for the ^{174}Yb and ^{176}Yb samples.

overcompensation was removed by reducing the respective correction factor in the isotope correction matrix by 9.0%. For all other samples this effect was not observed.

Following the correction for isotopic impurities, the background due to capture of sample scattered neutrons was removed from the spectra by means of the data measured with the scattering sample. Except for ^{174}Yb and ^{176}Yb, this correction is very small due to the favorable ratios of total and capture cross sections for most isotopes. It was obtained in the same way as described in the samarium measurement [1]. After this last correction, the final spectra contain only the net capture events of the investigated

Table 6: MATRIX FOR ISOTOPIC CORRECTIONS (%)

Corrected spectrum	Measured spectrum						Corrected sample thickness
	^{170}Yb	^{171}Yb	^{172}Yb	^{173}Yb	^{174}Yb	^{176}Yb	(10^{-3} at/barn)
^{170}Yb	100	−34.780	−6.806	−4.981	−1.310	−0.352	2.8015
^{171}Yb	−0.382	100	−2.349	−0.854	−0.220	−0.024	1.3820
^{172}Yb	+0.010	−1.744	100	−7.968	−0.779	−0.118	4.6440
^{173}Yb	−0.022	−0.359	−1.342	100	−3.053	−0.093	2.2189
^{174}Yb	−0.105	−0.822	−0.436	−2.039	100	−0.847	7.6618
^{176}Yb	−0.261	−2.799	−1.312	−2.333	−2.388	100	7.3499

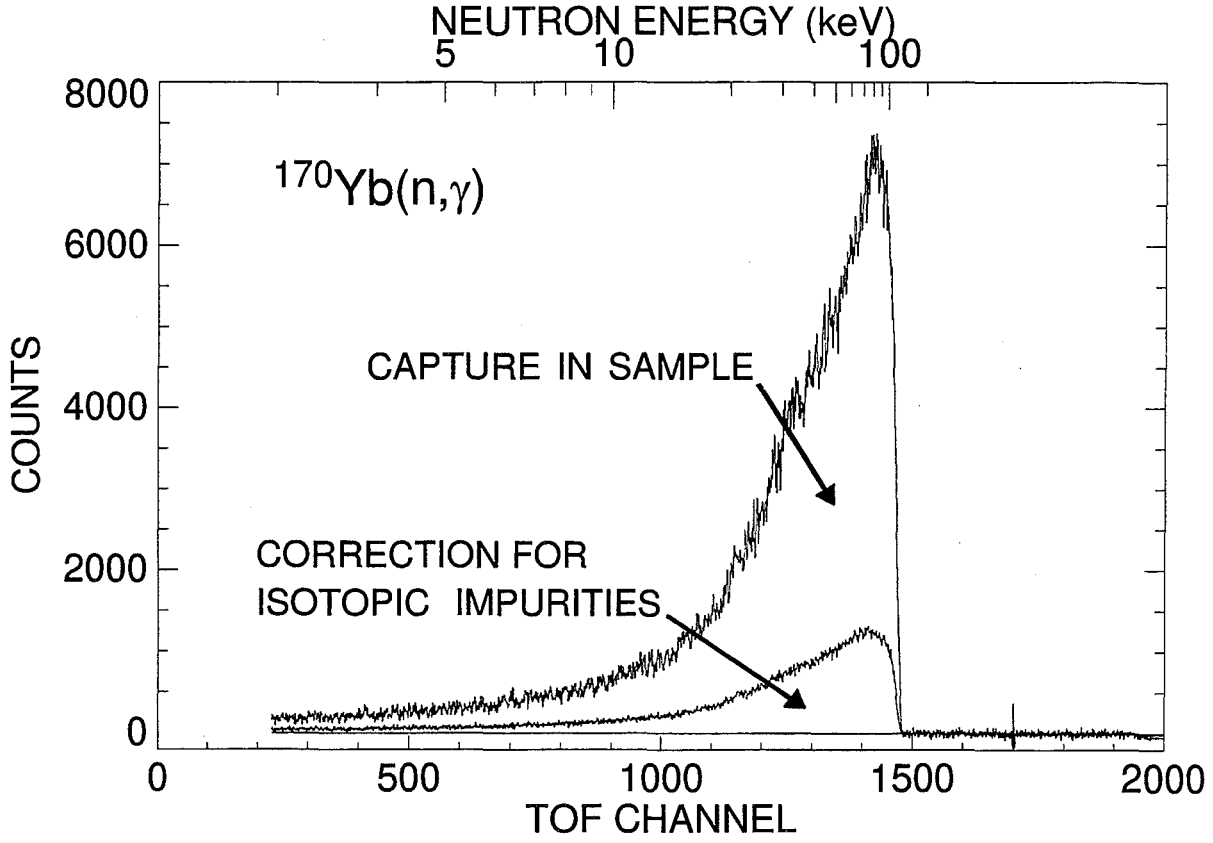

Figure 5: TOF spectrum of the ^{170}Yb sample. The background due to isotopic impurities is shown separately.

isotopes (bottom spectra in Figs. 2, 3, and 4). The corrections for capture of scattered neutrons are shown for all measured isotopes in Fig. 6, and the corresponding signal/background ratios are listed in Table 7 for different neutron energies.

Table 7: SIGNAL/BACKGROUND RATIO FOR RUNS WITH DIFFERENT MAXIMUM NEUTRON ENERGY

Sample	σ_t/σ_γ[a]	Maximum neutron energy	Signal/Background ratio[b]		
	E_n=30 keV	(keV)	E_n=30 keV	E_n=20 keV	E_n=10 keV
^{170}Yb	24	100	8.2	3.5	2.4
^{171}Yb	13		8.8	4.3	2.2
^{172}Yb	47		5.4	2.6	1.8
^{173}Yb	21		6.8	3.6	2.1
^{174}Yb	110		3.7	2.0	1.3
^{176}Yb	131		3.4	1.9	1.5
^{197}Au	24		9.3	4.4	3.1
^{170}Yb		200	5.2	2.9	2.0
^{171}Yb			5.9	3.3	1.9
^{172}Yb			3.8	2.3	1.6
^{173}Yb			5.0	2.9	1.8
^{174}Yb			3.1	2.0	1.3
^{176}Yb			2.9	1.8	1.3
^{197}Au			7.7	3.8	2.7

[a]Total cross section including oxygen
[b]Defined as (effect+neutron scattering background)/(neutron scattering background)

After subtraction of the scattering background the cross section shape versus neutron energy was determined from the TOF spectra of Fig. 6. For normalization, the two-dimensional data were projected onto the sum energy axis using the TOF region with optimum signal/background ratio as indicated in Fig. 6 by dashed boxes. The resulting pulse height spectra are shown in Fig. 7 for the events with multiplicity >2. The threshold in sum energy is 1.6 MeV.

Signals from the $4\pi BaF_2$ detector are only accepted as capture events, if they coincide within a resolving time of ~10ns. Thus, capture cascades leading to an isomeric state do not contain the full binding energy of the captured neutron, and the respective events are registered at correspondingly lower energies. As shown in Fig. 7, the isomeric states in the even ytterbium isotopes 172 to 176 are high enough, that this effect is clearly resolved within the energy resolution of the $4\pi BaF_2$ detector. With the ground state spin increasing from 5/2 (^{173}Yb) to 9/2 (^{177}Yb) the 1/2 isomers are populated with increasing intensity. In neutron capture of ^{173}Yb the 6^+ isomer in ^{174}Yb is weakly populated, too. Only in ^{171}Yb, the isomeric state is too low to be resolved in the present experiment.

The sum energy spectra of all isotopes are shown in Fig. 8 for different multiplicities. These multiplicities correspond to the number of detector modules contributing per event, which are slightly larger than the true multiplicities because of cross talking. In the even

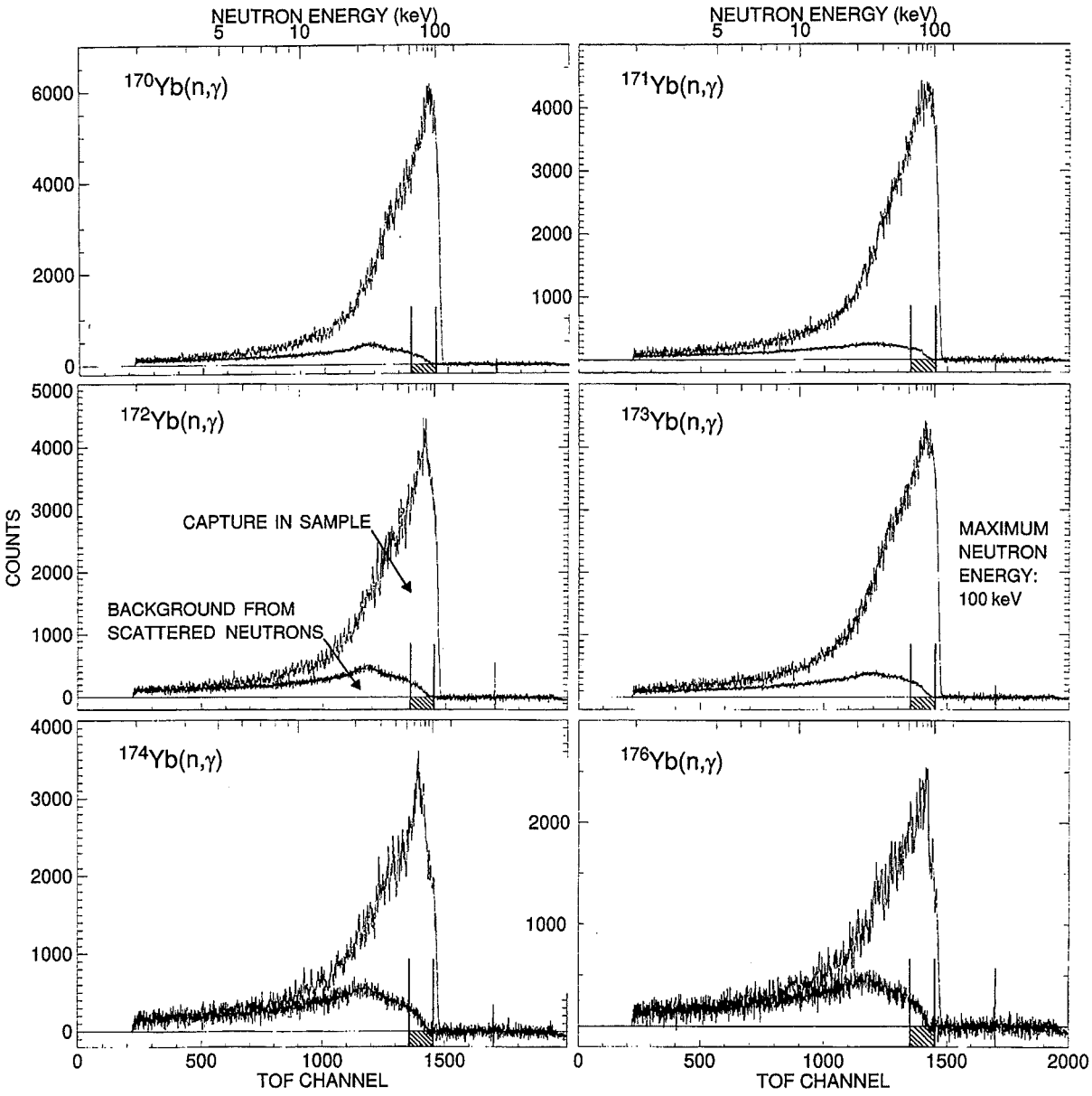

Figure 6: TOF spectra measured with the ytterbium samples in Run III (100 keV maximum neutron energy). The background due to sample scattered neutrons is shown separately. The region used for absolute normalization of the cross section is indicated by hatched boxes.

ytterbium isotopes, 20 to 30% of the capture events are observed with multiplicities ≥ 5, while the respective fraction in the odd isotopes is about 40–45%. Note, that different multiplicity distributions for neutron captures feeding the ground and isomeric states are clearly observed for ^{172}Yb and ^{174}Yb. The arrows in Fig. 8 indicate the range of sum energy channels that were integrated to obtain the TOF spectra of Fig. 6 for determining the cross section shapes.

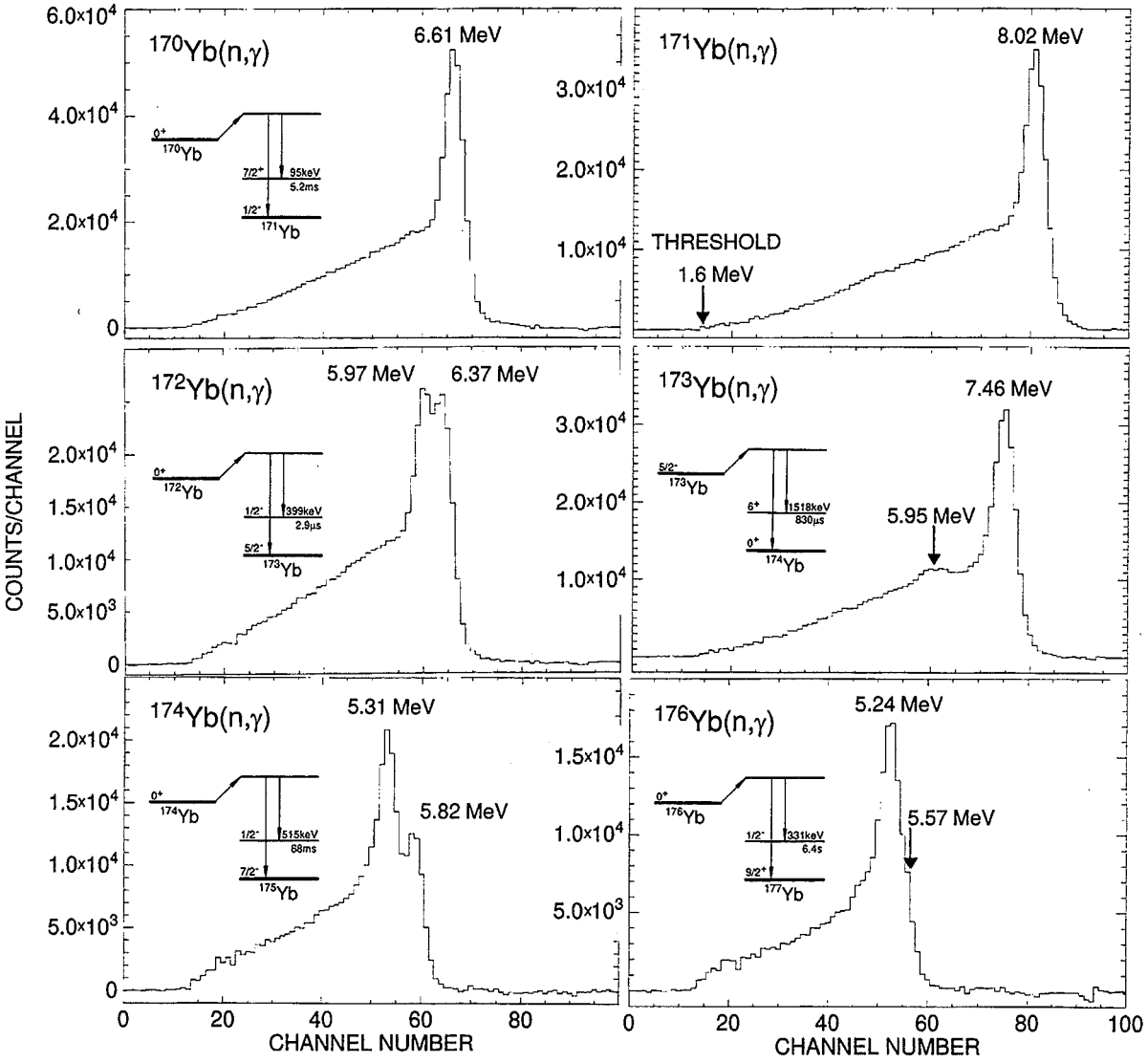

Figure 7: Sum energy spectra of all isotopes measured in Run III containing events with multiplicity >2. These spectra were obtained by projection of the two-dimensional spectra in the TOF region below the maximum neutron energy as indicated by hatched boxes in Fig. 6. The insets indicate the decay schemes to ground and isomeric states.

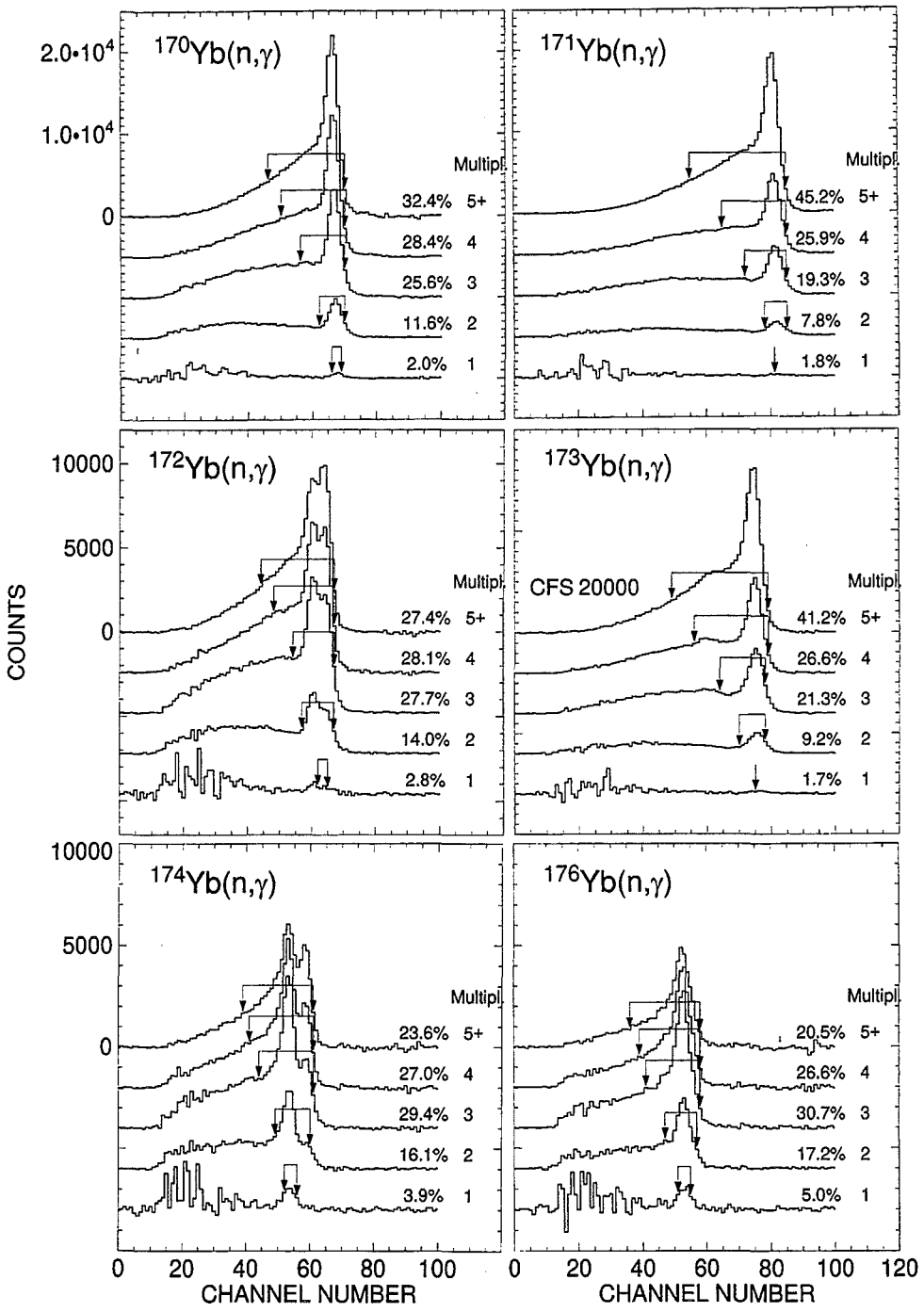

Figure 8: Sum energy spectra of all isotopes as a function of multiplicity. The regions used to determine the cross section shape are indicated by arrows. Note that capture events feeding the ground and isomeric states in ^{172}Yb and ^{174}Yb exhibit very different multiplicity distributions.

The cross section ratio of isotope X relative to the gold standard is given by

$$\frac{\sigma_i(X)}{\sigma_i(Au)} = \frac{Z_i(X)}{Z_i(Au)} \cdot \frac{\Sigma Z(Au)}{\Sigma Z(X)} \cdot \frac{\Sigma E(X)}{\Sigma E(Au)} \cdot \frac{m(Au)}{m(X)} \cdot F_1 \cdot F_2. \quad (1)$$

In this expression, Z_i is the count rate of channel i in the TOF spectrum, ΣZ is the TOF rate integrated over the interval used for normalization (hatched box in Fig. 6), ΣE is the total count rate in the sum energy spectra for all multiplicities in this TOF interval. The respective sum energy spectra are shown in Fig. 8. For all multiplicities these spectra were integrated from the threshold at 1.6 MeV beyond the binding energy, and the sum of these results, ΣE is used in Eq. 1. A full description of this procedure is given in Ref.[21]. The quantity m is the sample thickness in atoms/barn. The factor F_1 = (100–f(Au))/(100–f(X)) corrects for the fraction of capture events f below the experimental threshold in sum energy, where X refers to the respective ytterbium sample (Table 8), and F_2 is the ratio of the multiple scattering and self–shielding corrections.

The fraction of unobserved capture events, f, and the correction factor F_1 were calculated as described in Ref. [17]. The input for this calculation are the individual neutron capture cascades and their relative contributions to the total capture cross section as well as the detector efficiency for monoenergetic γ–rays in the energy range up to 10 MeV. As in the experiment on dysprosium isotopes [4] this information was derived directly from the experimental data recorded with the ADC system in Run III. From these data, only events close to the sum energy peak (see Fig. 7) were selected, which contained the full capture γ–ray cascade. This ensemble was further reduced by restricting the analysis to the TOF region with optimum signal to background ratio (dashed areas in Fig. 6). The correction factors F_1 were calculated as described in Ref. [17] and are quoted in Table 8. As in all previous experiments with the 4π BaF_2 detector, F_1 was found to depend linearly on the binding energy of the captured neutron; only for ^{176}Yb a ~1% deviation was found from this relation.

The capture γ-ray spectra deduced from the data taken with the ADC system are shown in Fig. 9 in energy bins of 500 keV. The spectra show neither the significant structure around 2-3 MeV nor the pronounced soft component observed in case of the dysprosium isotopes [4].

The correction for neutron multiple scattering and self–shielding was calculated with the SESH code [18]. Apart from the pairing energies [22], most of the input parameters were taken from Ref. [23] but were slightly modified in order to reproduce the measured total and capture cross sections. The final values are listed in Table 9 together with the calculated total cross sections. The resulting correction factors, MS(X) and F_2, are compiled in Tables 10 and 11.

Since the enrichment of some samples is comparably low, these corrections were calculated either for the true sample composition or for that part which remains after the correction for isotopic impurities. It was assumed, that subtraction of the isotopic impurities via the normalized spectra of the other samples accounts for the respective contributions to the multiple scattering corrections as well. Therefore, the cross section was determined using the corrections calculated as if the samples consisted of the main isotopes only. In general, these corrections are below 5% except for the even isotopes at energies below 10 keV.

Table 8: FRACTION OF UNDETECTED CAPTURE EVENTS, f (%), AND THE RELATED CORRECTION FACTORS F_1.[a]

	Threshold in Sum Energy (MeV)			
	1.5	1.6	1.75	2.0
f(Au)	4.97			6.92
f(^{170}Yb)	2.17			3.45
f(^{171}Yb)	1.28			2.04
f(^{172}Yb)	2.44			3.97
f(^{173}Yb)	1.56			2.62
f(^{174}Yb)	3.42			5.34
f(^{176}Yb)	5.02			7.51
F_1(^{170}Yb/Au)	0.971	0.970	0.968	0.964
F_1(^{171}Yb/Au)	0.963	0.960	0.957	0.950
F_1(^{172}Yb/Au)	0.974	0.973	0.972	0.969
F_1(^{173}Yb/Au)	0.965	0.963	0.961	0.956
F_1(^{174}Yb/Au)	0.984	0.984	0.984	0.983
F_1(^{176}Yb/Au)	1.001	1.002	1.004	1.006

[a] derived from capture cascades measured with the ADC system.

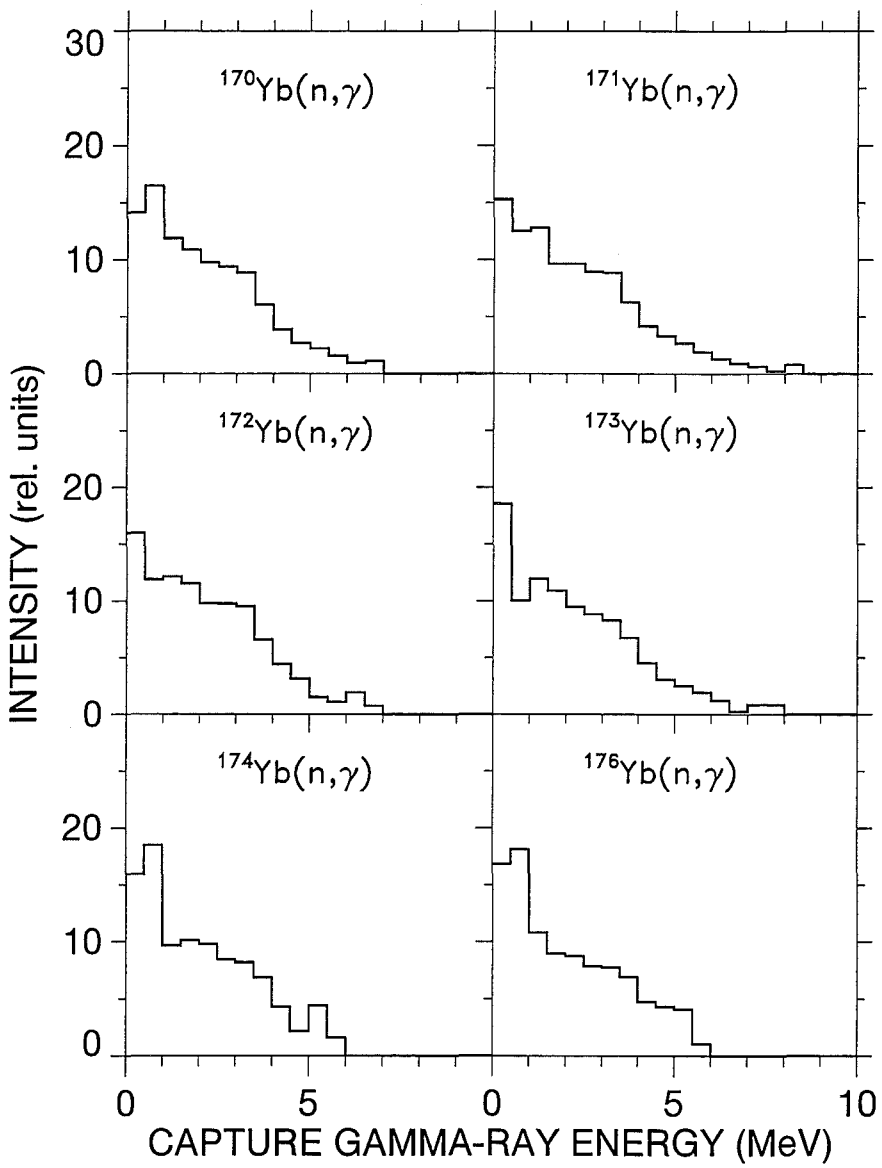

Figure 9: Capture γ-ray spectra derived from the capture cascades recorded with the ADC system.

Table 9: PARAMETERS FOR THE CALCULATION OF NEUTRON SELF-SHIELDING AND MULTIPLE SCATTERING CORRECTIONS

Parameter		^{170}Yb	^{171}Yb	^{172}Yb	^{173}Yb	^{174}Yb	^{176}Yb	^{16}O
Nucleon Number		170	171	172	173	174	176	16
Binding Energy (MeV)		6.614	8.020	6.367	7.465	5.822	5.567	4.144
Pairing Energy (MeV)		0.68	1.37	0.68	1.23	0.68	0.68	2.5
Effective Temperature (K)		293	293	293	293	293	293	293
Nuclear Spin		0	0.5	0	2.5	0	0	0
Average Radiation	s	0.140	0.120	0.090	0.090	0.065	0.060	0.0
Width (eV)	p	0.100	0.060	0.060	0.060	0.040	0.020	–
	d	0.020	0.020	0.020	0.020	0.020	0.020	–
Average Level	s	37.	5.8	70.0	7.8	162.	180.	10^6
Spacing (eV)	p[a]	12.3	2.6	23.3	3.9	54.0	60.	–
	d[a]	7.4	1.5	14.0	2.6	32.4	36.	–
Strength Function	S_0	2.4	1.7	1.7	1.7	1.6	1.8	0.0
(10^{-4})	S_1	0.94	0.86	0.82	0.78	0.74	0.60	–
	S_2	3.0	2.9	2.7	2.6	2.5	2.4	–
Nuclear Radius	s	7.3	7.3	7.4	7.4	7.9	7.3	5.5
(fm)	p	7.3	7.3	7.4	7.4	7.9	7.3	–
	d	7.3	7.3	7.4	7.4	7.9	7.3	–
		Calculated total cross sections						
3 keV		24.7	19.5	19.7	19.7	19.8	20.2	3.80
5 keV		20.6	16.6	16.8	16.7	17.1	17.1	3.80
10 keV		16.4	13.6	13.8	13.8	14.3	13.9	3.79
20 keV		13.4	11.5	11.6	11.6	12.2	11.6	3.77
40 keV		11.1	9.90	10.0	10.0	10.6	9.91	3.74
80 keV		9.39	8.69	8.79	8.76	9.34	8.57	3.68
160 keV		8.04	7.75	7.81	7.77	8.25	7.51	3.55
320 keV		7.11	7.14	7.14	7.09	7.40	6.81	3.31

[a]Calculated with SESH [18]

Table 10: CORRECTION FACTORS FOR NEUTRON SELF-SHIELDING AND MULTIPLE SCATTERING, MS

Energy Bin	MS						
(keV)	^{197}Au	^{170}Yb	^{171}Yb	^{172}Yb	^{173}Yb	^{174}Yb	^{176}Yb
3 – 5	0.995	0.913	1.007	0.857	1.001	0.780	0.727
5 – 7.5	1.016	0.958	1.014	0.922	1.012	0.865	0.810
7.5 – 10	1.027	0.982	1.017	0.960	1.018	0.920	0.856
10 – 12.5	1.032	0.996	1.018	0.981	1.020	0.945	0.890
12.5 –15	1.035	1.004	1.018	0.991	1.021	0.960	0.915

Table 10 (continued)

15 – 20	1.037	1.010	1.018	1.004	1.022	0.975	0.938
20 – 25	1.037	1.016	1.018	1.012	1.022	0.985	0.960
25 – 30	1.036	1.018	1.018	1.016	1.022	0.990	0.970
30 – 40	1.036	1.020	1.018	1.018	1.022	0.995	0.980
40 – 50	1.035	1.021	1.017	1.019	1.022	1.000	0.986
50 – 60	1.034	1.021	1.017	1.019	1.022	1.000	0.994
60 – 80	1.033	1.020	1.017	1.018	1.021	1.005	1.000
80 – 100	1.032	1.020	1.016	1.018	1.021	1.005	1.002
100 – 120	1.030	1.019	1.016	1.018	1.021	1.007	1.005
120 – 150	1.029	1.018	1.016	1.018	1.020	1.008	1.006
150 – 175	1.028	1.018	1.015	1.018	1.020	1.010	1.007
175 – 200	1.027	1.017	1.015	1.017	1.020	1.012	1.007
200 – 225	1.026	1.017	1.015	1.017	1.019	1.015	1.010
Uncertainty (%)	0.3	0.4	0.2	0.3	0.2	0.7	1.0

Table 11: CORRECTION FACTORS FOR THE CROSS SECTION RATIOS, F_2 = MS(Au)/MS(X)

Energy Bin	F_2					
(keV)	^{170}Yb/Au	^{171}Yb/Au	^{172}Yb/Au	^{173}Yb/Au	^{174}Yb/Au	^{176}Yb/Au
3 – 5	1.090	0.988	1.161	0.994	1.276	1.369
5 – 7.5	1.061	1.002	1.102	1.004	1.175	1.254
7.5– 10	1.046	1.010	1.070	1.009	1.116	1.200
10 – 12.5	1.036	1.014	1.052	1.012	1.092	1.160
12.5 – 15	1.031	1.017	1.044	1.014	1.078	1.131
15 – 20	1.027	1.019	1.033	1.015	1.064	1.106
20 – 25	1.021	1.019	1.025	1.015	1.053	1.080
25 – 30	1.018	1.018	1.020	1.014	1.046	1.068
30 – 40	1.016	1.018	1.018	1.014	1.041	1.057
40 – 50	1.014	1.018	1.016	1.013	1.035	1.050
50 – 60	1.013	1.017	1.015	1.012	1.034	1.040
60 – 80	1.013	1.016	1.015	1.012	1.028	1.033
80 – 100	1.012	1.016	1.014	1.011	1.027	1.030
100 – 120	1.011	1.014	1.012	1.009	1.023	1.025
120 – 150	1.011	1.013	1.011	1.009	1.021	1.023
150 – 175	1.010	1.013	1.010	1.008	1.018	1.021
175 – 200	1.010	1.012	1.010	1.007	1.015	1.020
200 – 225	1.009	1.011	1.009	1.007	1.011	1.016
Uncertainty (%)	0.5	0.4	0.4	0.4	0.8	1.1

4 RESULTS FOR THE NEUTRON CAPTURE CROSS SECTIONS

The measured neutron capture cross section ratios of the investigated Yb isotopes, and of ^{197}Au are listed in Tables 12 to 17 together with the respective statistical uncertainties. The data are given for all runs and for the two evaluation methods discussed in Sec. 3. The last column in each table contains the weighted average, the weight being determined by the inverse of the squared statistical uncertainties. Since the cross section ratios depend weakly on energy, the averages for the energy interval from 30 to 80 keV are also included for a better comparison of the individual results. The data are free of systematic differences with respect to different runs or evaluations. This is important as they were obtained with different data acquisition modes and neutron spectra.

As in the previous measurements with the 4π BaF_2 detector [1, 15, 24], the final cross section ratios were adopted from Evaluation 2. The respective mean values are compiled for all runs in Table 18 together with the statistical, systematic, and total uncertainties. The energy bins are sufficiently fine to avoid systematic uncertainties in the calculation of the Maxwellian averaged cross sections (Sec. 6). The final uncertainties of the cross section ratios are less than 1.4% in the energy range from 15 to 100 keV for all isotopes except ^{176}Yb, but reach 10 to 20% in the lowest energy bin of the ^{174}Yb and ^{176}Yb cross sections, respectively.

The experimental ratios were converted into absolute cross sections using the gold data of Macklin [25] after normalization by a factor of 0.989 to the absolute value of Ratynski and Käppeler [26] (Table 19). The uncertainties of the resulting values can be obtained by adding the 1.5% uncertainty of the reference cross section to the uncertainties of the respective cross section ratios.

The present results are compared to previous data in Figs. 10 to 12. In general, the present results are systematically lower than the previous cross sections. At least part of this discrepancy can be related to the effect of capture to isomeric states which was not considered in the older data. Comparably good agreement is found with the data of Beer et al. for ^{170}Yb. The results of Shorin et al. for ^{176}Yb are the only ones beeing systematically lower. The uncertainties of the present data are much smaller than in all previous measurements.

Table 12: $\sigma(^{170}\mathrm{Yb})/\sigma(^{197}\mathrm{Au})$ AND STATISTICAL UNCERTAINTIES IN (%)

Energy Bin (keV)	Run I		Run II		Run III		Average	
Evaluation 1								
3 – 5	1.0032	7.7	1.0086	14.	1.0188	7.3	1.0111	4.9
5 – 7.5	1.0076	4.7	0.9119	7.1	1.0073	3.9	0.9928	2.8
7.5 – 10	1.0937	3.7	1.1201	5.7	1.1712	3.3	1.1342	2.3
10 – 12.5	1.1255	2.8	1.1515	3.8	1.1883	2.5	1.1587	1.7
12.5 – 15	1.1559	2.5	1.2029	3.6	1.1984	2.3	1.1834	1.5
15 – 20	1.1873	1.6	1.2437	2.1	1.2518	1.4	1.2279	1.0
20 – 25	1.4485	1.4	1.4272	1.7	1.4268	1.2	1.4339	0.8
25 – 30	1.3481	1.2	1.3662	1.3	1.3859	1.0	1.3693	0.7
30 – 40	1.4314	1.0	1.4220	0.9	1.4494	0.8	1.4362	0.5
40 – 50	1.5227	1.1	1.5025	0.9	1.5377	0.8	1.5228	0.5
50 – 60	1.5151	1.0	1.5323	1.0	1.5538	0.8	1.5376	0.5
60 – 80	1.5632	0.9	1.5775	0.8	1.5719	0.7	1.5718	0.5
80 – 100	1.5069	1.0	1.4984	0.8	1.5357	0.7	1.5162	0.5
100 – 120	1.3293	1.0	1.3613	0.8	1.3492	0.9	1.3495	0.5
120 – 150	–	–	1.2250	0.7	–	–	1.2250	0.7
150 – 175	–	–	1.1913	0.8	–	–	1.1913	0.8
175 – 200	–	–	1.1345	0.9	–	–	1.1345	0.9
200 – 225	–	–	1.0913	1.4	–	–	1.0913	1.4
30 – 80	1.5081	0.9	1.5086	0.5	1.5282	0.6	1.5153	0.4
Evaluation 2								
3 – 5	0.9811	6.1	0.8642	10.	0.9181	5.4	0.9350	3.8
5 – 7.5	1.0060	3.4	1.0336	5.1	0.9832	3.0	0.9995	2.1
7.5 – 10	1.0969	2.8	1.1543	4.1	1.1284	2.5	1.1210	1.7
10 – 12.5	1.1870	2.2	1.1579	3.0	1.1912	2.0	1.1832	1.3
12.5 – 15	1.2007	2.0	1.2421	2.8	1.1976	1.8	1.2070	1.2
15 – 20	1.2240	1.2	1.2773	1.7	1.2473	1.1	1.2447	0.7
20 – 25	1.4543	1.1	1.4418	1.3	1.4170	1.0	1.4362	0.6
25 – 30	1.3547	0.9	1.3745	1.1	1.3766	0.9	1.3681	0.5
30 – 40	1.4418	0.7	1.4246	0.8	1.4349	0.7	1.4347	0.4
40 – 50	1.5122	0.7	1.5137	0.8	1.5177	0.7	1.5147	0.4
50 – 60	1.5034	0.7	1.5295	0.8	1.5266	0.7	1.5187	0.4
60 – 80	1.5589	0.6	1.5725	0.7	1.5458	0.6	1.5576	0.3
80 – 100	1.4923	0.6	1.4885	0.7	1.5027	0.6	1.4952	0.4
100 – 120	1.3190	0.7	1.3446	0.7	1.3241	0.8	1.3296	0.4
120 – 150	–	–	1.2132	0.7	–	–	1.2132	0.7
150 – 175	–	–	1.1754	0.7	–	–	1.1754	0.7
175 – 200	–	–	1.1178	0.8	–	–	1.1178	0.8
200 – 225	–	–	1.0658	1.3	–	–	1.0658	1.3
30 – 80	1.5041	0.5	1.5101	0.4	1.5063	0.4	1.5072	0.3

Table 13: $\sigma(^{171}\mathrm{Yb})/\sigma(^{197}\mathrm{Au})$ AND STATISTICAL UNCERTAINTIES IN (%)

Energy Bin (keV)	Run I		Run II		Run III		Average	
Evaluation 1								
3 – 5	1.4516	9.7	1.8341	16.	1.6962	8.5	1.6240	6.0
5 – 7.5	1.6413	5.5	1.6642	8.1	1.6448	4.7	1.6468	3.3
7.5 – 10	1.8270	4.3	1.8660	6.7	1.9205	3.9	1.8768	2.6
10 – 12.5	1.7312	3.3	1.6886	4.8	1.8420	3.0	1.7747	2.0
12.5 – 15	1.8890	2.8	1.9430	4.2	1.9493	2.6	1.9256	1.7
15 – 20	1.9746	1.8	2.0877	2.4	2.0528	1.6	2.0323	1.1
20 – 25	2.3216	1.6	2.3625	1.9	2.3709	1.3	2.3529	0.9
25 – 30	2.2510	1.3	2.2439	1.5	2.3442	1.1	2.2902	0.7
30 – 40	2.1918	1.1	2.1529	1.0	2.2339	0.8	2.1991	0.6
40 – 50	2.4156	1.1	2.3775	1.0	2.4577	0.9	2.4227	0.6
50 – 60	2.4433	1.1	2.4576	1.0	2.5099	0.8	2.4777	0.6
60 – 80	2.2981	1.0	2.3273	0.8	2.3749	0.7	2.3419	0.5
80 – 100	2.1301	1.0	2.1306	0.9	2.1931	0.7	2.1579	0.5
100 – 120	1.8904	1.1	1.8858	0.9	1.9500	0.9	1.9093	0.6
120 – 150	–	–	1.6552	0.8	–	–	1.6552	0.8
150 – 175	–	–	1.4987	0.9	–	–	1.4987	0.9
175 – 200	–	–	1.4181	1.0	–	–	1.4181	1.0
200 – 225	–	–	1.3036	1.8	–	–	1.3036	1.8
30 – 80	2.3372	0.9	2.3288	0.6	2.3941	0.6	2.3570	0.4
Evaluation 2								
3 – 5	1.4789	7.3	1.6317	11.	1.6585	6.0	1.5931	4.3
5 – 7.5	1.6773	3.9	1.7065	6.0	1.6955	3.4	1.6905	2.4
7.5 – 10	1.8112	3.2	1.8285	4.9	1.9258	2.8	1.8681	1.9
10 – 12.5	1.8270	2.5	1.7486	3.6	1.9097	2.2	1.8509	1.5
12.5 – 15	1.9821	2.2	2.0026	3.2	2.0142	2.0	2.0002	1.3
15 – 20	2.0503	1.3	2.1161	1.9	2.0885	1.2	2.0794	0.8
20 – 25	2.3385	1.1	2.3328	1.5	2.3384	1.1	2.3372	0.7
25 – 30	2.2416	0.9	2.2620	1.2	2.3030	0.9	2.2707	0.6
30 – 40	2.2179	0.7	2.1619	0.9	2.2198	0.7	2.2046	0.4
40 – 50	2.4096	0.7	2.4022	0.9	2.4265	0.7	2.4143	0.4
50 – 60	2.4440	0.7	2.4780	0.9	2.4623	0.7	2.4593	0.4
60 – 80	2.3121	0.6	2.3411	0.7	2.3415	0.6	2.3311	0.4
80 – 100	2.1318	0.6	2.1261	0.7	2.1607	0.6	2.1413	0.4
100 – 120	1.8849	0.8	1.8879	0.8	1.9186	0.8	1.8961	0.5
120 – 150	–	–	1.6508	0.7	–	–	1.6508	0.7
150 – 175	–	–	1.4961	0.8	–	–	1.4961	0.8
175 – 200	–	–	1.4075	0.9	–	–	1.4075	0.9
200 – 225	–	–	1.2893	1.5	–	–	1.2893	1.5
30 – 80	2.3459	0.5	2.3458	0.5	2.3625	0.4	2.3532	0.3

Table 14: $\sigma(^{172}\mathrm{Yb})/\sigma(^{197}\mathrm{Au})$ AND STATISTICAL UNCERTAINTIES IN (%)

Energy Bin (keV)	Run I		Run II		Run III		Average	
Evaluation 1								
3 – 5	0.4518	10.	0.4101	20.	0.4216	10.	0.4339	6.7
5 – 7.5	0.4262	6.1	0.4301	8.9	0.4593	5.0	0.4435	3.6
7.5 – 10	0.5549	4.2	0.5855	6.3	0.6058	3.7	0.5837	2.5
10 – 12.5	0.4796	3.4	0.4537	5.0	0.5043	3.1	0.4864	2.1
12.5 – 15	0.5043	2.9	0.5394	4.2	0.5311	2.7	0.5226	1.8
15 – 20	0.5861	1.8	0.6301	2.3	0.6021	1.6	0.6023	1.1
20 – 25	0.6756	1.5	0.6832	1.9	0.6865	1.3	0.6821	0.9
25 – 30	0.6085	1.3	0.6101	1.5	0.6390	1.1	0.6223	0.8
30 – 40	0.6315	1.1	0.6287	1.0	0.6468	0.9	0.6372	0.6
40 – 50	0.6776	1.1	0.6732	1.1	0.6896	0.9	0.6815	0.6
50 – 60	0.6794	1.1	0.6770	1.1	0.7017	0.9	0.6887	0.6
60 – 80	0.7186	1.0	0.7333	0.9	0.7332	0.7	0.7298	0.5
80 – 100	0.5877	1.0	0.5869	0.9	0.5997	0.8	0.5927	0.5
100 – 120	0.5084	1.1	0.5172	0.9	0.5138	1.0	0.5137	0.6
120 – 150	–	–	0.4704	0.9	–	–	0.4704	0.9
150 – 175	–	–	0.4359	0.9	–	–	0.4359	0.9
175 – 200	–	–	0.4197	1.0	–	–	0.4197	1.0
200 – 225	–	–	0.4000	1.8	–	–	0.4000	1.8
30 – 80	0.6768	0.9	0.6781	0.6	0.6928	0.6	0.6839	0.4
Evaluation 2								
3 – 5	0.4570	7.8	0.3401	16.	0.3896	7.4	0.4138	5.1
5 – 7.5	0.4356	4.4	0.4506	6.8	0.4382	3.8	0.4391	2.6
7.5 – 10	0.5577	3.1	0.5765	4.8	0.5652	2.8	0.5642	1.9
10 – 12.5	0.5030	2.6	0.4818	3.8	0.4982	2.4	0.4971	1.6
12.5 – 15	0.5258	2.3	0.5558	3.3	0.5303	2.1	0.5332	1.4
15 – 20	0.5864	1.3	0.6265	1.9	0.6003	1.3	0.6002	0.8
20 – 25	0.6796	1.1	0.6770	1.5	0.6785	1.1	0.6785	0.7
25 – 30	0.6168	1.0	0.6160	1.3	0.6328	0.9	0.6230	0.6
30 – 40	0.6316	0.7	0.6310	0.9	0.6338	0.7	0.6323	0.4
40 – 50	0.6739	0.8	0.6811	0.9	0.6792	0.7	0.6778	0.5
50 – 60	0.6715	0.7	0.6749	0.9	0.6859	0.7	0.6781	0.4
60 – 80	0.7139	0.6	0.7284	0.8	0.7178	0.6	0.7190	0.4
80 – 100	0.5810	0.7	0.5841	0.8	0.5852	0.6	0.5835	0.4
100 – 120	0.5022	0.8	0.5113	0.8	0.5031	0.9	0.5056	0.5
120 – 150	–	–	0.4655	0.8	–	–	0.4655	0.8
150 – 175	–	–	0.4289	0.9	–	–	0.4289	0.9
175 – 200	–	–	0.4141	1.0	–	–	0.4141	1.0
200 – 225	–	–	0.3893	1.6	–	–	0.3893	1.6
30 – 80	0.6727	0.5	0.6789	0.5	0.6792	0.5	0.6769	0.3

Table 15: $\sigma(^{173}\mathrm{Yb})/\sigma(^{197}\mathrm{Au})$ AND STATISTICAL UNCERTAINTIES IN (%)

Energy Bin (keV)	Run I		Run II		Run III		Average	
Evaluation 1								
3 – 5	1.1947	8.1	1.2594	15.	1.2362	7.6	1.2220	5.2
5 – 7.5	1.1127	5.1	1.0063	7.9	1.0326	4.6	1.0587	3.1
7.5 – 10	1.2275	4.0	1.2688	6.2	1.2285	3.7	1.2346	2.5
10 – 12.5	1.1471	3.1	1.0806	4.6	1.1826	2.9	1.1514	1.9
12.5 – 15	1.2590	2.7	1.2905	4.0	1.3001	2.5	1.2828	1.7
15 – 20	1.2977	1.7	1.3499	2.3	1.3605	1.5	1.3362	1.0
20 – 25	1.4609	1.5	1.4838	1.8	1.4861	1.3	1.4773	0.9
25 – 30	1.3862	1.3	1.4011	1.5	1.4238	1.1	1.4063	0.7
30 – 40	1.3783	1.1	1.3673	1.0	1.3781	0.8	1.3749	0.6
40 – 50	1.4357	1.1	1.4020	1.0	1.4494	0.9	1.4319	0.6
50 – 60	1.3830	1.1	1.3966	1.1	1.4293	0.8	1.4079	0.6
60 – 80	1.3786	1.0	1.3887	0.9	1.4035	0.7	1.3931	0.5
80 – 100	1.2632	1.0	1.2476	0.9	1.2810	0.7	1.2659	0.5
100 – 120	1.1334	1.1	1.1469	0.9	1.1455	0.9	1.1429	0.6
120 – 150	–	–	1.0669	0.8	–	–	1.0669	0.8
150 – 175	–	–	0.9985	0.9	–	–	0.9985	0.9
175 – 200	–	–	0.9406	1.0	–	–	0.9406	1.0
200 – 225	–	–	0.8553	1.7	–	–	0.8553	1.7
30 – 80	1.3939	0.9	1.3887	0.6	1.4151	0.6	1.4004	0.4
Evaluation 2								
3 – 5	1.2065	6.1	1.2828	9.7	1.1958	5.3	1.2124	3.7
5 – 7.5	1.0872	3.6	1.0341	5.8	1.0421	3.2	1.0578	2.2
7.5 – 10	1.2047	2.9	1.2719	4.4	1.2265	2.7	1.2258	1.8
10 – 12.5	1.1916	2.4	1.1212	3.3	1.2159	2.1	1.1899	1.4
12.5 – 15	1.3102	2.0	1.3266	3.0	1.3264	1.9	1.3203	1.3
15 – 20	1.3420	1.3	1.3788	1.8	1.3619	1.2	1.3577	0.8
20 – 25	1.4580	1.1	1.4762	1.4	1.4616	1.0	1.4634	0.7
25 – 30	1.3863	0.9	1.4039	1.2	1.4113	0.9	1.4003	0.6
30 – 40	1.3804	0.7	1.3758	0.8	1.3720	0.7	1.3759	0.4
40 – 50	1.4227	0.7	1.4213	0.9	1.4343	0.7	1.4269	0.4
50 – 60	1.3756	0.7	1.4058	0.9	1.4052	0.7	1.3946	0.4
60 – 80	1.3802	0.6	1.3897	0.7	1.3824	0.6	1.3834	0.4
80 – 100	1.2566	0.6	1.2433	0.7	1.2586	0.6	1.2539	0.4
100 – 120	1.1306	0.8	1.1462	0.8	1.1275	0.8	1.1350	0.5
120 – 150	–	–	1.0607	0.7	–	–	1.0607	0.7
150 – 175	–	–	0.9925	0.8	–	–	0.9925	0.8
175 – 200	–	–	0.9279	0.9	–	–	0.9279	0.9
200 – 225	–	–	0.8371	1.5	–	–	0.8371	1.5
30 – 80	1.3897	0.5	1.3982	0.5	1.3985	0.4	1.3959	0.3

Table 16: $\sigma(^{174}\mathrm{Yb})/\sigma(^{197}\mathrm{Au})$ AND STATISTICAL UNCERTAINTIES IN (%)

Energy Bin (keV)	Run I		Run II		Run III		Average	
Evaluation 1								
3 – 5	0.1627	28.	0.2828	26.	0.2998	15.	0.2726	12.
5 – 7.5	0.1234	20.	0.1701	18.	0.2059	10.	0.1855	8.1
7.5 – 10	0.1752	11.	0.2146	12.	0.2263	7.6	0.2103	5.6
10 – 12.5	0.2069	6.7	0.2094	8.4	0.2523	5.1	0.2307	3.6
12.5 – 15	0.2400	5.0	0.2614	6.4	0.2600	4.3	0.2536	2.9
15 – 20	0.2674	2.8	0.2660	3.7	0.2809	2.5	0.2731	1.7
20 – 25	0.3051	2.3	0.3101	2.8	0.3003	2.0	0.3042	1.3
25 – 30	0.2756	1.9	0.2764	2.3	0.2906	1.7	0.2824	1.1
30 – 40	0.2887	1.5	0.2819	1.6	0.2960	1.2	0.2902	0.8
40 – 50	0.2893	1.5	0.2872	1.7	0.2943	1.3	0.2909	0.8
50 – 60	0.3083	1.4	0.3123	1.6	0.3182	1.2	0.3137	0.8
60 – 80	0.3179	1.3	0.3260	1.4	0.3281	1.0	0.3246	0.7
80 – 100	0.2142	1.4	0.2113	1.5	0.2189	1.2	0.2155	0.8
100 – 120	0.1858	1.6	0.1901	1.6	0.1956	1.5	0.1907	0.9
120 – 150	–	–	0.1665	1.5	–	–	0.1665	1.5
150 – 175	–	–	0.1552	1.6	–	–	0.1552	1.6
175 – 200	–	–	0.1471	1.8	–	–	0.1471	1.8
200 – 225	–	–	0.1495	3.1	–	–	0.1495	3.1
30 – 80	0.3011	1.2	0.3019	1.1	0.3092	0.9	0.3050	0.6
Evaluation 2								
3 – 5	0.1645	23.	0.2274	23.	0.2717	12.	0.2462	9.5
5 – 7.5	0.1349	14.	0.1711	15.	0.1774	8.6	0.1668	6.6
7.5 – 10	0.1942	7.6	0.2201	9.2	0.2195	5.8	0.2122	4.1
10 – 12.5	0.2216	5.1	0.2185	6.4	0.2527	3.9	0.2370	2.8
12.5 – 15	0.2476	4.0	0.2570	5.2	0.2568	3.4	0.2538	2.3
15 – 20	0.2766	2.2	0.2805	2.9	0.2783	2.0	0.2781	1.3
20 – 25	0.3112	1.7	0.3073	2.2	0.3003	1.6	0.3057	1.0
25 – 30	0.2833	1.4	0.2898	1.8	0.2911	1.3	0.2881	0.9
30 – 40	0.2886	1.1	0.2899	1.4	0.2919	1.0	0.2903	0.6
40 – 50	0.2888	1.1	0.2932	1.4	0.2912	1.0	0.2908	0.7
50 – 60	0.3077	1.0	0.3144	1.4	0.3127	1.0	0.3112	0.6
60 – 80	0.3168	0.9	0.3271	1.2	0.3236	0.8	0.3219	0.5
80 – 100	0.2129	1.0	0.2129	1.3	0.2140	0.9	0.2134	0.6
100 – 120	0.1854	1.2	0.1904	1.3	0.1912	1.3	0.1889	0.7
120 – 150	–	–	0.1668	1.3	–	–	0.1668	1.3
150 – 175	–	–	0.1563	1.4	–	–	0.1563	1.4
175 – 200	–	–	0.1460	1.6	–	–	0.1460	1.6
200 – 225	–	–	0.1470	2.6	–	–	0.1470	2.6
30 – 80	0.3005	0.8	0.3062	1.0	0.3049	0.7	0.3037	0.5

Table 17: $\sigma(^{176}\mathrm{Yb})/\sigma(^{197}\mathrm{Au})$ AND STATISTICAL UNCERTAINTIES IN (%)

Energy Bin (keV)	Run I		Run II		Run III		Average	
Evaluation 1								
3 – 5	0.1450	34.	0.1915	39.	0.0802	58.	0.1510	24.
5 – 7.5	0.1680	16.	0.1613	20.	0.1554	14.	0.1612	9.4
7.5 – 10	0.1973	10.	0.2439	11.	0.2078	9.1	0.2137	5.9
10 – 12.5	0.1602	8.6	0.1593	11.	0.1954	6.8	0.1775	4.8
12.5 – 15	0.1884	6.3	0.1940	8.2	0.2017	5.7	0.1954	3.7
15 – 20	0.1915	3.7	0.2017	4.6	0.1945	3.5	0.1951	2.2
20 – 25	0.2179	2.8	0.2218	3.4	0.2119	2.7	0.2165	1.7
25 – 30	0.2346	2.2	0.2414	2.5	0.2525	1.9	0.2438	1.3
30 – 40	0.2077	1.8	0.1998	2.0	0.2143	1.6	0.2085	1.0
40 – 50	0.2369	1.7	0.2282	2.0	0.2383	1.5	0.2353	1.0
50 – 60	0.2315	1.7	0.2286	2.0	0.2403	1.5	0.2345	1.0
60 – 80	0.2413	1.5	0.2387	1.7	0.2486	1.3	0.2438	0.9
80 – 100	0.1720	1.7	0.1714	1.8	0.1797	1.4	0.1751	0.9
100 – 120	0.1383	2.0	0.1382	2.0	0.1399	2.0	0.1388	1.2
120 – 150	–	–	0.1224	1.9	–	–	0.1224	1.9
150 – 175	–	–	0.1114	2.0	–	–	0.1114	2.0
175 – 200	–	–	0.0983	2.4	–	–	0.0983	2.4
200 – 225	–	–	0.0983	4.4	–	–	0.0983	4.4
30 – 80	0.2294	1.4	0.2238	1.4	0.2354	1.2	0.2302	0.8
Evaluation 2								
3 – 5	0.1339	30.	0.1301	41.	0.1138	30.	0.1251	19.
5 – 7.5	0.1416	14.	0.1598	16.	0.1457	12.	0.1478	7.9
7.5 – 10	0.2177	7.3	0.2457	8.6	0.2235	6.3	0.2268	4.2
10 – 12.5	0.1898	6.1	0.1743	7.8	0.1951	5.2	0.1890	3.5
12.5 – 15	0.2013	4.9	0.2121	6.0	0.1968	4.4	0.2019	2.9
15 – 20	0.1981	2.9	0.1983	3.7	0.1923	2.7	0.1957	1.7
20 – 25	0.2250	2.2	0.2272	2.7	0.2069	2.1	0.2183	1.3
25 – 30	0.2410	1.6	0.2518	2.0	0.2476	1.5	0.2462	1.0
30 – 40	0.2102	1.3	0.2045	1.7	0.2092	1.2	0.2085	0.8
40 – 50	0.2388	1.3	0.2364	1.6	0.2330	1.2	0.2358	0.8
50 – 60	0.2319	1.3	0.2346	1.6	0.2333	1.2	0.2331	0.8
60 – 80	0.2425	1.1	0.2423	1.4	0.2422	1.0	0.2423	0.7
80 – 100	0.1728	1.2	0.1735	1.5	0.1745	1.1	0.1737	0.7
100 – 120	0.1378	1.5	0.1396	1.7	0.1353	1.6	0.1376	0.9
120 – 150	–	–	0.1235	1.6	–	–	0.1235	1.6
150 – 175	–	–	0.1126	1.7	–	–	0.1126	1.7
175 – 200	–	–	0.1022	2.0	–	–	0.1022	2.0
200 – 225	–	–	0.0973	3.6	–	–	0.0973	3.6
30 – 80	0.2309	0.9	0.2295	1.2	0.2294	0.8	0.2300	0.5

Table 18: FINAL NEUTRON CAPTURE CROSS SECTION RATIOS OF ^{170}Yb, ^{171}Yb, ^{172}Yb, ^{173}Yb ^{174}Yb, AND ^{176}Yb RELATIVE TO ^{197}Au

Energy Bin[a]	$\frac{\sigma(^{170}Yb)}{\sigma(^{197}Au)}$	Uncertainty (%)			$\frac{\sigma(^{171}Yb)}{\sigma(^{197}Au)}$	Uncertainty (%)			$\frac{\sigma(^{172}Yb)}{\sigma(^{197}Au)}$	Uncertainty (%)		
(keV)		stat	sys	tot		stat	sys	tot		stat	sys	tot
3 – 5	0.9350	3.8	0.9	3.9	1.5931	4.3	0.9	4.4	0.4138	5.1	0.8	5.2
5 – 7.5	0.9995	2.1	0.9	2.3	1.6905	2.4	0.9	2.6	0.4391	2.6	0.8	2.7
7.5 – 10	1.1210	1.7	0.9	1.9	1.8681	1.9	0.9	2.1	0.5642	1.9	0.8	2.1
10 – 12.5	1.1832	1.3	0.9	1.6	1.8509	1.5	0.9	1.7	0.4971	1.6	0.8	1.8
12.5 – 15	1.2070	1.2	0.9	1.5	2.0002	1.3	0.9	1.6	0.5332	1.4	0.8	1.6
15 – 20	1.2447	0.7	0.9	1.1	2.0794	0.8	0.9	1.2	0.6002	0.8	0.8	1.1
20 – 25	1.4362	0.6	0.9	1.1	2.3372	0.7	0.9	1.1	0.6785	0.7	0.8	1.1
25 – 30	1.3681	0.5	0.9	1.0	2.2707	0.6	0.9	1.1	0.6230	0.6	0.8	1.0
30 – 40	1.4347	0.4	0.9	1.0	2.2046	0.4	0.9	1.0	0.6323	0.4	0.8	0.9
40 – 50	1.5147	0.4	0.9	1.0	2.4143	0.4	0.9	1.0	0.6778	0.5	0.8	0.9
50 – 60	1.5187	0.4	0.9	1.0	2.4593	0.4	0.9	1.0	0.6781	0.4	0.8	0.9
60 – 80	1.5576	0.3	0.9	0.9	2.3311	0.4	0.9	1.0	0.7190	0.4	0.8	0.9
80 – 100	1.4952	0.4	0.9	1.0	2.1413	0.4	0.9	1.0	0.5835	0.4	0.8	0.9
100 – 120	1.3296	0.4	0.9	1.0	1.8961	0.5	0.9	1.0	0.5056	0.5	0.8	0.9
120 – 150	1.2132	0.7	0.9	1.1	1.6508	0.7	0.9	1.1	0.4655	0.8	0.8	1.1
150 – 175	1.1754	0.7	0.9	1.1	1.4961	0.8	0.9	1.2	0.4289	0.9	0.8	1.2
175 – 200	1.1178	0.8	0.9	1.2	1.4075	0.9	0.9	1.3	0.4141	1.0	0.8	1.3
200 – 225	1.0658	1.3	0.9	1.6	1.2893	1.5	0.9	1.7	0.3893	1.6	0.8	1.8

Energy Bin[a]	$\frac{\sigma(^{173}Yb)}{\sigma(^{197}Au)}$	Uncertainty (%)			$\frac{\sigma(^{174}Yb)}{\sigma(^{197}Au)}$	Uncertainty (%)			$\frac{\sigma(^{176}Yb)}{\sigma(^{197}Au)}$	Uncertainty (%)		
(keV)		stat	sys	tot		stat	sys	tot		stat	sys	tot
3 – 5	1.2124	3.7	0.9	3.8	0.2462	9.5	1.0	9.6	0.1251	19.	1.6	19.
5 – 7.5	1.0578	2.2	0.9	2.4	0.1668	6.6	1.0	6.7	0.1478	7.9	1.6	8.1
7.5 – 10	1.2258	1.8	0.9	2.0	0.2122	4.1	1.0	4.2	0.2268	4.2	1.6	4.5
10 –12.5	1.1899	1.4	0.9	1.7	0.2370	2.8	1.0	3.0	0.1890	3.5	1.6	3.8
12.5 – 15	1.3203	1.3	0.9	1.6	0.2538	2.3	1.0	2.5	0.2019	2.9	1.6	3.3
15 – 20	1.3577	0.8	0.9	1.2	0.2781	1.3	1.0	1.6	0.1957	1.7	1.6	2.3
20 – 25	1.4634	0.7	0.9	1.1	0.3057	1.0	1.0	1.4	0.2183	1.3	1.6	2.1
25 – 30	1.4003	0.6	0.9	1.1	0.2881	0.9	1.0	1.3	0.2462	1.0	1.6	1.9
30 – 40	1.3759	0.4	0.9	1.0	0.2903	0.6	1.0	1.2	0.2085	0.8	1.6	1.8
40 – 50	1.4269	0.4	0.9	1.0	0.2908	0.7	1.0	1.2	0.2358	0.8	1.6	1.8
50 – 60	1.3946	0.4	0.9	1.0	0.3112	0.6	1.0	1.2	0.2331	0.8	1.6	1.8
60 – 80	1.3834	0.4	0.9	1.0	0.3219	0.5	1.0	1.1	0.2423	0.7	1.6	1.7
80 – 100	1.2539	0.4	0.9	1.0	0.2134	0.6	1.0	1.2	0.1737	0.7	1.6	1.7
100 – 120	1.1350	0.5	0.9	1.0	0.1889	0.7	1.0	1.2	0.1376	0.9	1.6	1.8
120 – 150	1.0607	0.7	0.9	1.1	0.1668	1.3	1.0	1.6	0.1235	1.6	1.6	2.3
150 – 175	0.9925	0.8	0.9	1.2	0.1563	1.4	1.0	1.7	0.1126	1.7	1.6	2.3
175 – 200	0.9279	0.9	0.9	1.3	0.1460	1.6	1.0	1.9	0.1022	2.0	1.6	2.6
200 – 225	0.8371	1.5	0.9	1.7	0.1470	2.6	1.0	2.8	0.0973	3.6	1.6	3.9

[a] Energy bins as used for calculating the Maxwellian averaged cross sections

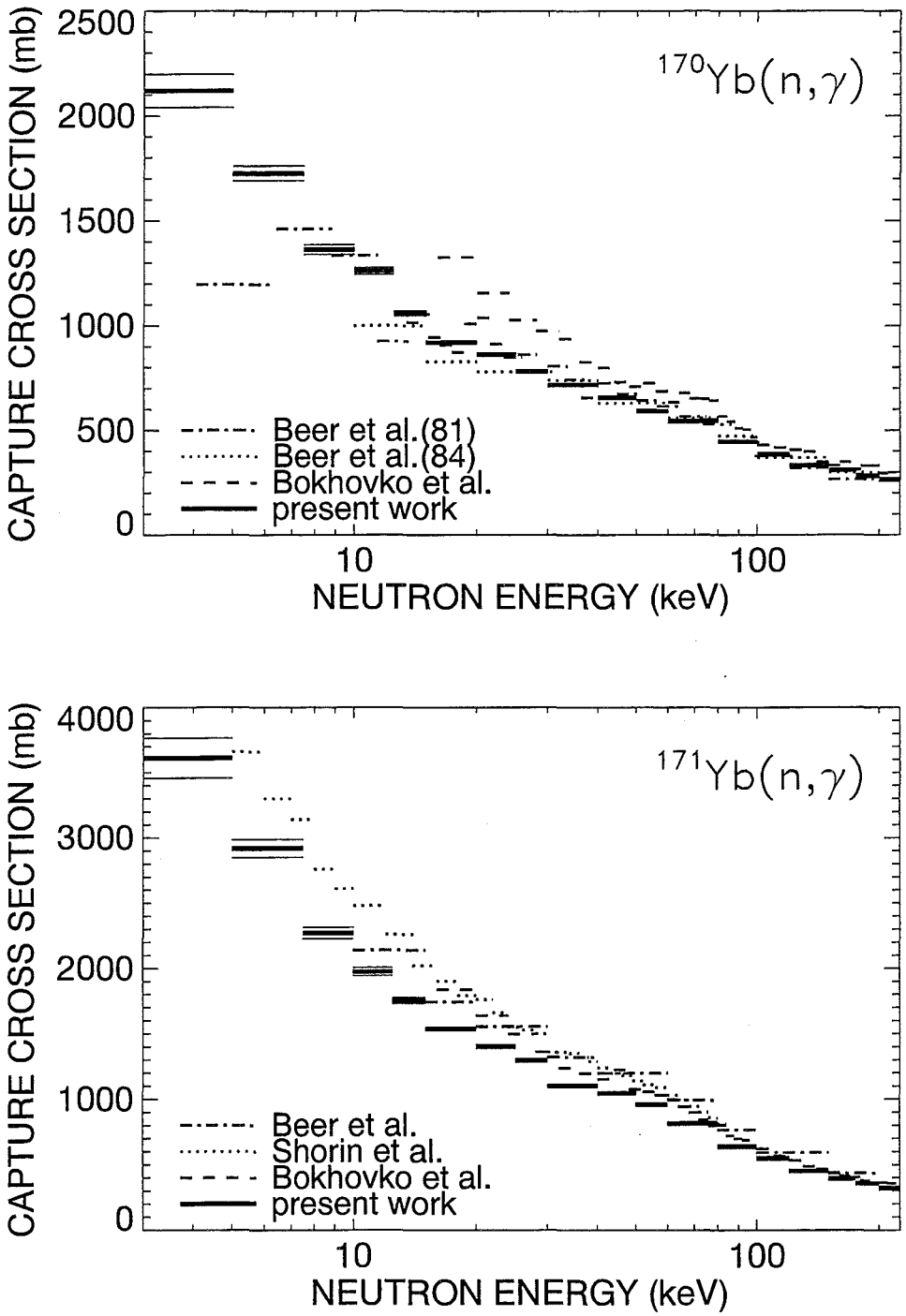

Figure 10: The neutron capture cross sections of ^{170}Yb and ^{171}Yb compared to previous data [9, 10, 11, 12].

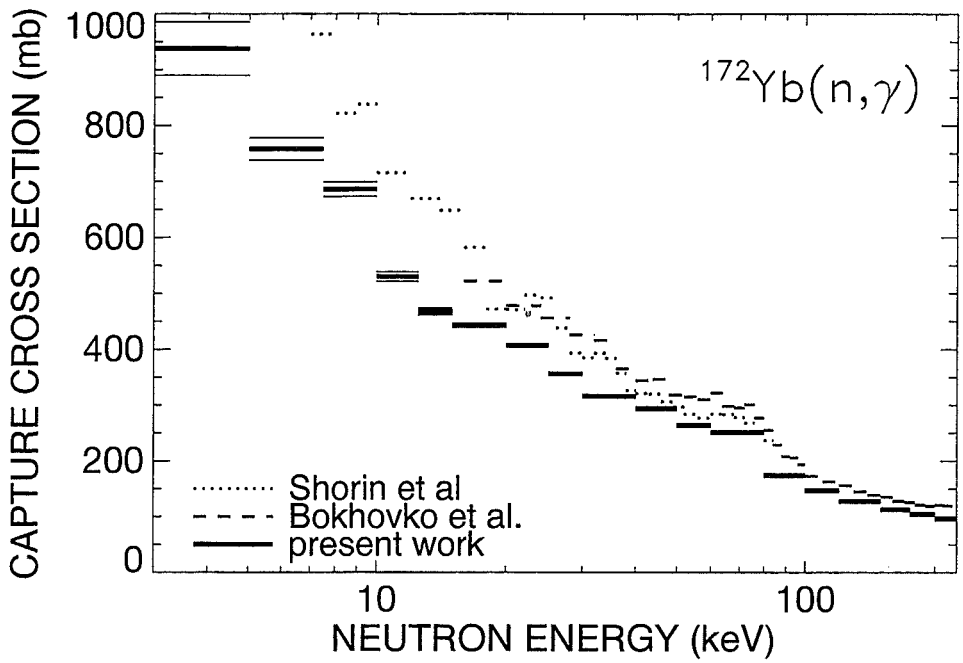

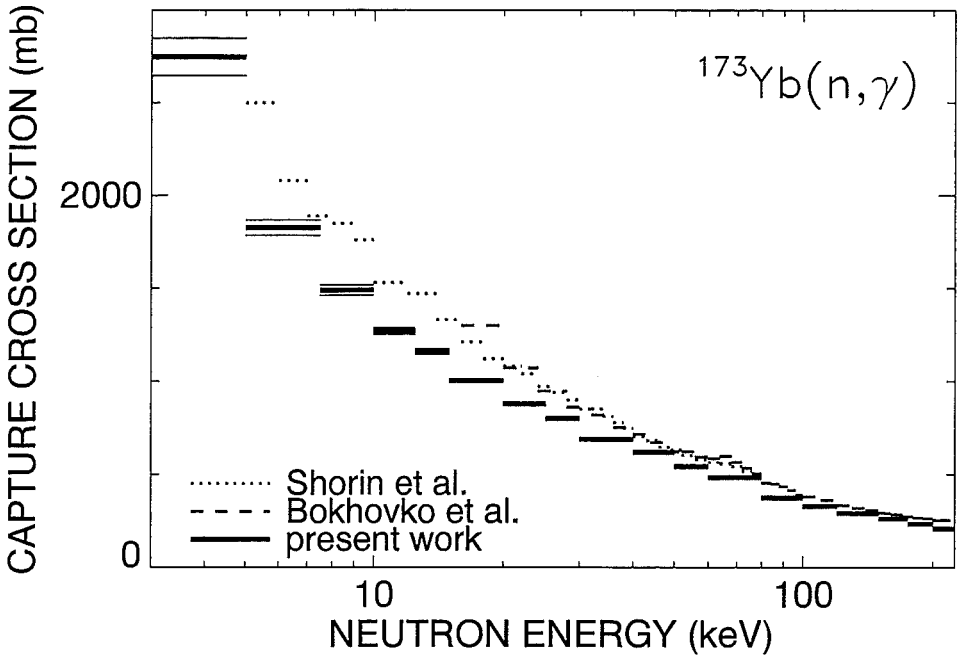

Figure 11: The neutron capture cross sections of ^{172}Yb and ^{173}Yb compared to previous data [9, 10].

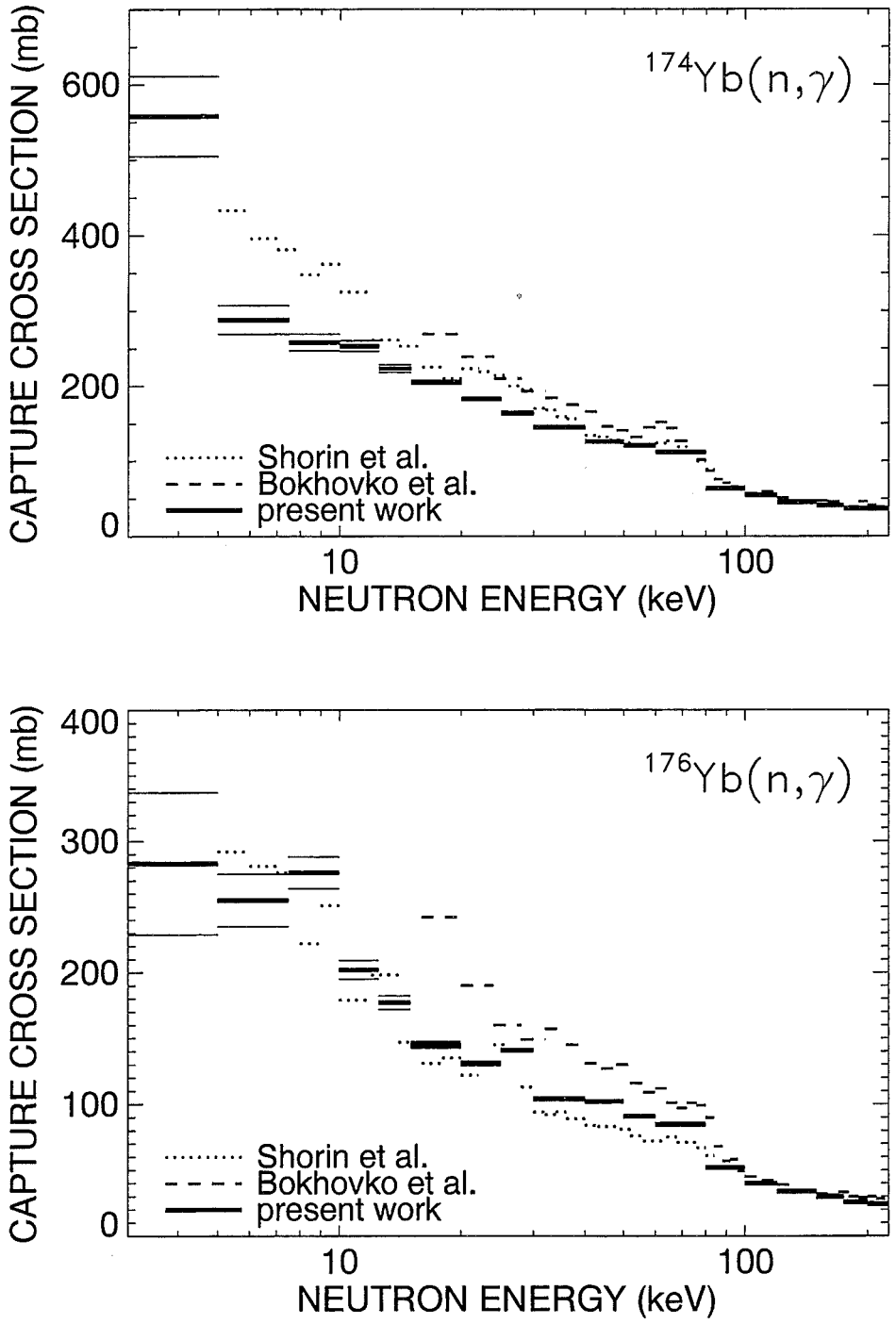

Figure 12: The neutron capture cross sections of ^{174}Yb and ^{176}Yb compared to previous data [9, 10].

Table 19: NEUTRON CAPTURE CROSS SECTIONS OF ^{170}Yb, ^{171}Yb,^{172}Yb, ^{173}Yb, ^{174}Yb, AND ^{176}Yb (in mb).

Energy Bin[a] (keV)	$\sigma(^{197}Au)^b$	$\sigma(^{170}Yb)$	$\sigma(^{171}Yb)$	$\sigma(^{172}Yb)$	$\sigma(^{173}Yb)$	$\sigma(^{174}Yb)$	$\sigma(^{176}Yb)$
3 – 5	2266.7	2119.	3611.	938.1	2748.	558.0	283.5
5 – 7.5	1726.7	1726.	2919.	758.2	1827.	288.0	255.3
7.5 – 10	1215.7	1363.	2271.	685.9	1490.	258.0	275.8
10 – 12.5	1066.7	1262.	1974.	530.2	1269.	252.8	201.7
12.5 – 15	878.0	1060.	1756.	468.1	1159.	222.8	177.3
15 – 20	738.8	919.5	1536.	443.4	1003.	205.5	144.6
20 – 25	600.0	861.8	1402.	407.1	878.1	183.4	131.0
25 – 30	570.8	780.9	1296.	355.6	799.3	164.4	140.6
30 – 40	500.4	717.9	1103.	316.4	688.5	145.3	104.3
40 – 50	433.3	656.4	1046.	293.7	618.3	126.0	102.2
50 – 60	389.6	591.7	958.2	264.2	543.4	121.3	90.8
60 – 80	349.4	544.2	814.4	251.2	483.3	112.5	84.7
80 – 100	298.3	446.0	638.8	174.1	374.0	63.7	51.8
100 – 120	290.1	385.8	550.1	146.7	329.3	54.8	39.9
120 – 150	274.1	332.6	452.5	127.6	290.8	45.7	33.9
150 – 175	263.7	309.9	394.5	113.1	261.7	41.2	29.7
175 – 200	252.6	282.3	355.5	104.6	234.4	36.9	25.8
200 – 225	248.5	264.8	320.4	96.7	208.0	36.5	24.2

[a]As used for calculating the Maxwellian averaged cross sections
[b]Based on the ^{197}Au data from literature[25, 26]

5 DISCUSSION OF UNCERTAINTIES

The determination of statistical and systematic uncertainties in measurements with the 4π BaF_2 detector has been described in Refs. [1, 15, 17]. The following discussion emphasizes the particular aspects of the present experiment. The various uncertainties are compiled in Table 20.

The binding energy for all investigated isotopes is sufficiently low for normalizing the scattering background in the sum energy region around 9 MeV. Therefore, no systematic differences were observed in the data, neither between individual runs nor correlated with the different acquisition modes or evaluation methods (see Tables 12 to 17). This implies that systematic uncertainties in background subtraction were negligible as in the measurements on the samarium [1], gadolinium [2], and dysprosium [4] isotopes. For the scattering correction, this could be confirmed via the pulse height spectra measured at low neutron energies, where the absence of any (positive or negative) structure around 9

MeV γ–ray energy due to neutron captures in the odd barium isotopes verifies the correct treatment of the scattering background.

The systematic uncertainties related to the flight path measurement and the neutron flux normalization have been discussed previously and are given in Table 20.

The problem of admixtures of other rare earth elements, especially of europium with its very high cross section, has been discussed in detail for ^{142}Nd and ^{144}Nd [28]. Since this background concerns isotopes with small cross sections, it has to be considered mainly for ^{174}Yb and ^{176}Yb. In contrast to previous measurements no contaminations of other rare earth elements were detected in the present samples and only upper limits for a few elements were found in chemical analyses: Er (<0.03%), Tm (<0.01%) and Lu (<0.01%) for the ^{176}Yb sample and Er (<0.005%), Tm (<0.005%) and Lu (<0.04%) for the ^{174}Yb sample. From these limits, systematic cross section uncertainties of less than 0.2% were obtained, an estimate that was adopted for all investigated isotopes.

The isotopic composition (Table 2) was specified with an absolute uncertainty of <0.2% for the main isotope and of <0.1% for the impurity isotopes in each sample. In view of the very good agreement with the independently measured isotopic composition of the neodymium samples [3] these seem to be rather conservative estimates. Nevertheless, this information was adopted in the analysis, resulting in a relative uncertainty of 0.2% for the mass of the main isotopes in the highly enriched samples. For the less enriched ^{170}Yb sample, however, an uncertainty of 0.3% had to be assumed instead.

The uncertainty of the isotopic correction has been discussed in detail for the gadolinium and dysprosium isotopes [2], [4]. Following this discussion, for the small isotopic corrections in the present experiment uncertainties of 0.2% are estimated for all isotopes.

Samples with low enrichment are also problematic with respect to the correction for multiple scattering and self–shielding. Subtraction of the normalized spectra of the impurity isotopes may either be insufficient or may even overcompensate the multiple scattering effect. This holds if sizable corrections are required and if the individual sample masses are significantly different as in case of the ^{170}Yb and ^{171}Yb samples. Accordingly, the overcompensation was clearly visible in the sum energy spectrum and required the renormalization of this correction (Sec. 3). For all other samples the effect was not visible in the spectra but may still cause a small uncertainty. Therefore, the calculation of the correction factors MS were performed twice, before and after the correction for isotopic impurities. The respective differences were 1.3% for the ^{170}Yb sample, 0.8% for the ^{176}Yb sample, and less than 0.5% in all other cases, nearly independent of neutron energy. In analogy to the gadolinium experiment [2], 25% of this difference were adopted as the related systematic uncertainty and were added to the uncertainties provided by the SESH code [18].

The systematic uncertainties due to undetected events were discussed in detail for the gadolinium experiment [2], where uncertainties of 0.3% for the even and 0.8% for the odd isotopes were estimated for the correction factor F_1. This estimate was based on two independent sets of calculated capture cascades, and was found to agree with the respective uncertainties quoted in previous measurements with the 4π BaF_2 detector [1, 15, 24]. It turned out that this uncertainty was mainly determined by the difference in binding energy between the investigated isotope and the gold standard, which is large for the odd, but small for the even gadolinium isotopes. For ytterbium the same effect

Table 20: SYSTEMATIC UNCERTAINTIES (%)

Flight path	0.1
Neutron flux normalization	0.2
Sample mass: elemental impurities	0.2
Isotopic composition (^{170}Yb/other Yb samples)	0.3/0.2
Isotopic correction	0.2
Multiple scattering and self–shielding: F_2	
cross section ratio (^{176}Yb/^{174}Yb/^{170}Yb/others)	1.1/0.8/0.6/0.4
Undetected events: F_1	
cross section ratio (^{176}Yb/^{171,173}Yb/^{172,174}Yb/^{170}Yb)	1.1/0.7/0.5/0.4
total systematic uncertainties	
$\sigma(^{170}\mathrm{Yb})/\sigma(\mathrm{Au})$	0.9
$\sigma(^{171}\mathrm{Yb})/\sigma(\mathrm{Au})$	0.9
$\sigma(^{172}\mathrm{Yb})/\sigma(\mathrm{Au})$	0.8
$\sigma(^{173}\mathrm{Yb})/\sigma(\mathrm{Au})$	0.9
$\sigma(^{174}\mathrm{Yb})/\sigma(\mathrm{Au})$	1.0
$\sigma(^{176}\mathrm{Yb})/\sigma(\mathrm{Au})$	1.6

is observed. However, the differences are slightly larger for the even and lower for the odd isotopes, with different signs for odd and even nuclei. Therefore, uncertainties of 0.4% and 0.7% had to be assigned, respectively, similar to the dysprosium isotopes [4]. An additional uncertainty arises in the present experiment for ^{172}Yb, ^{174}Yb, and ^{176}Yb due to the strong population of isomeric states. The correction was calculated assuming that the capture cascades represent the full binding energy. Since the correction factor F_1 depends linearly on the binding energy, it is estimated to change by less than 0.3%, if an effective binding energy is used that accounts for the population of the isomer. Only for ^{176}Yb, the first isotope that showed a significant deviation from the linear dependence, this assumption might be too optimistic. Therefore, an additional systematic uncertainty of 1% was assumed in this case.

6 MAXWELLIAN AVERAGED CROSS SECTIONS

Maxwellian averaged cross sections were calculated in the same way as described in Refs. [15, 17]. The neutron energy range from 0 to 700 keV was divided into three intervals according to the origin of the adopted cross sections. The respective contributions I_x are given in Table 21. The main contribution, i.e. the interval I_2 from 3 to 225 keV, is provided by the present experiment (Table 19). These data were obtained with sufficient

resolution to exclude systematic uncertainties that may result from a coarse energy grid.

As in previous work, the contribution I_1 was determined in two ways. First, the cross sections were calculated from resonance parameters [23] and normalized to the results of the present experiment to avoid their original uncertainties. For the three isotopes ^{172}Yb, ^{174}Yb, and ^{176}Yb resonance parameters were available in the entire interval from 0 to 3 keV, while only restricted data up to 1 keV were known for the other isotopes. In these cases, the remaining gap was closed by a statistical model calculation. In the second approach the cross sections of Kopecky *et al.* [27] were normalized to the present data between 3 to 15 keV.

Both evaluations agreed to better than 6% for all isotopes, except for ^{173}Yb where a differenc of 14% was found. For the determination of the contribution to the Maxwellian averaged cross section, the mean of both evaluations was adopted with an uncertainty if $\pm$5%. Only for ^{173}Yb, this uncertainty had to be increased to $\pm$10%.

The energy interval from 225 to 700 keV contributes very little to the Maxwellian average at typical *s*–process temperatures. Here, the data of Bokhovko *et al.* [10] were used up to 460 keV neutron energy, normalized to the present results in the energy range from 100 to 225 keV, and in the remaining gap the shape of the data of Kopecky *et al.* [27] was used. The uncertainties were calculated as if the uncertainties of the normalized cross sections increased from 2% at 225 keV to 10% at 700 keV neutron energy.

The systematic uncertainties of the Maxwellian averaged cross sections in Table 21 correspond to the uncertainties of the cross section ratios (Table 18) and consider the respective I_1 and I_3 contributions. The 1.5% uncertainty of the gold standard was not included since it cancels out in most applications of relevance for *s*–process studies. In general, the systematic uncertainties dominate over the statistical uncertainties, except at low thermal energies.

The present results at kT=30 keV are eventually compared in Table 22 with previous experiments and with the compilations of Bao and Käppeler [29] and Beer, Voss, and Winters [30]. For the calculation of the Maxwellian average the data of Beer *et al.* [11][12], Shorin *et al.* [9] and Allen and Cohen [13] were corrected to compensate for differences in the adopted gold cross section [31]. Severe discrepancies are observed to most previous experiments. Reasonable agreement is found with the ^{170}Yb data of Beer *et al.* [12, 11] and of Allen and Cohen,[13], and with the data of Shorin *et al.* [9] for the higher ytterbium isotopes. Compared to the evaluated files, the present results for ^{171}Yb, ^{172}Yb, ^{173}Yb, and ^{174}Yb are lower by 15 to 20%, while agreement within 5% is only found for ^{170}Yb and ^{176}Yb.

Table 21: MAXWELLIAN AVERAGED NEUTRON CAPTURE CROSS SECTIONS OF THE YTERBIUM ISOTOPES.

^{170}Yb							
ΔE	0 - 3 keV	3 - 225 keV	225 - 700 keV	Thermal Spectrum			
Data:	see text	this work	from Ref. [10][a]				
kT	I_1	I_2	I_3	$<\sigma v>/v_T$ (mbarn)			
(keV)	(mbarn)	(mbarn)	(mbarn)		stat	sys[b]	tot
8	238.5±12.	1249.±9.7	0.0	1488.	15.	11.	19.
10	159.0±8.0	1163.±7.4	0.0	1322.	11.	10.	15.
15	74.6±3.7	1002.±4.6	0.0	1077.	5.9	9.0	11.
20	43.1±2.2	893.3±3.4	0.0	936.4	4.0	8.0	8.9
25	28.1±1.4	812.0±2.8	0.3	840.4	3.1	7.3	7.9
30	19.7±1.0	747.3±2.4	1.3	768.3	2.6	6.7	7.2
40	11.3±0.6	646.8±1.9	6.5±0.2	664.6	2.0	5.9	6.2
50	7.3±0.4	568.4±1.6	16.6±0.5	592.3	1.7	5.3	5.6
52	6.7±0.3	554.5±1.6	19.1±0.6	580.3	1.7	5.2	5.5
60	5.1±0.3	503.3±1.4	30.2±1.0	538.6	1.7	4.8	5.1
70	3.7±0.2	447.9±1.3	45.4±1.5	497.0	2.0	4.4	4.8
80	2.9±0.1	400.3±1.2	60.9±2.2	464.1	2.5	4.2	4.9
90	2.3±0.1	359.2±1.1	75.5±2.9	437.0	3.1	3.9	5.0
100	1.9±0.1	323.5±1.0	88.8±3.5	414.2	3.6	3.7	5.2
^{171}Yb							
ΔE	0 - 3 keV	3 - 225 keV	225 - 700 keV	Thermal Spectrum			
Data:	see text	this work	from Ref. [10][a]				
kT	I_1	I_2	I_3	$<\sigma v>/v_T$ (mbarn)			
(keV)	(mbarn)	(mbarn)	(mbarn)		stat	sys[b]	tot
8	406.5±20.	2064.±18.	0.0	2471.	27.	19.	33.
10	271.3±14.	1912.±14.	0.0	2183.	20.	17.	26.
15	127.9±6.4	1629.±8.5	0.0	1757.	11.	15.	19.
20	73.8±3.7	1435.±6.1	0.0	1509.	7.1	13.	15.
25	48.1±2.4	1290.±4.8	0.4	1339.	5.4	12.	13.
30	33.8±1.7	1175.±4.0	1.4	1210.	4.3	11.	12.
40	19.3±1.0	997.1±3.1	7.3±0.2	1024.	3.3	9.0	9.6
50	12.4±0.6	861.9±2.6	18.3±0.5	892.6	2.7	7.9	8.3
52	11.5±0.6	838.4±2.5	21.0±0.6	870.9	2.6	7.7	8.1
60	8.7±0.4	753.1±2.3	32.9±1.0	794.7	2.5	7.1	7.5
70	6.4±0.3	663.1±2.0	48.9±1.6	718.4	2.6	6.4	6.9
80	4.9±0.2	587.6±1.8	64.9±2.3	657.4	2.9	5.9	6.6
90	3.9±0.2	523.5±1.6	79.8±2.9	607.2	3.3	5.4	6.3
100	3.2±0.2	468.8±1.5	93.1±3.6	565.1	3.9	5.1	6.4

Table 21 (continued)

^{172}Yb							
ΔE	0 - 3 keV	3 - 225 keV	225 - 700 keV	Thermal Spectrum			
Data:	see text	this work	from Ref. [10][a]				
kT	I_1	I_2	I_3	$<\sigma v>/v_T$ (mbarn)			
(keV)	(mbarn)	(mbarn)	(mbarn)		stat	sys[b]	tot
8	103.4±5.2	569.4±5.6	0.0	672.8	7.6	4.6	8.9
10	69.0±3.5	530.4±4.2	0.0	599.4	5.5	4.2	6.9
15	32.4±1.6	456.0±2.6	0.0	488.4	3.1	3.6	4.8
20	18.8±0.9	403.9±1.8	0.0	422.7	2.0	3.2	3.8
25	12.2±0.6	364.2±1.5	0.1	376.5	1.6	2.9	3.3
30	8.6±0.4	332.2±1.2	0.5	341.3	1.3	2.7	3.0
40	4.9±0.2	282.5±1.0	2.3±0.1	289.7	1.0	2.3	2.5
50	3.2±0.2	244.5±0.8	6.0±0.2	253.7	0.8	2.0	2.2
52	2.9±0.1	237.8±0.8	6.9±0.2	247.6	0.8	2.0	2.2
60	2.2±0.1	213.8±0.7	10.8±0.3	226.8	0.8	1.8	2.0
70	1.6±0.1	188.4±0.6	16.2±0.5	206.2	0.8	1.6	1.8
80	1.3±0.1	167.0±0.6	21.7±0.8	190.0	1.0	1.5	1.8
90	1.0±0.1	148.9±0.5	26.8±1.0	176.7	1.1	1.4	1.8
100	0.8±0.0	133.4±0.5	31.5±1.2	165.7	1.3	1.3	1.8
^{173}Yb							
ΔE	0 - 3 keV	3 - 225 keV	225 - 700 keV	Thermal Spectrum			
Data:	see text	this work	from Ref. [10][a]				
kT	I_1	I_2	I_3	$<\sigma v>/v_T$ (mbarn)			
(keV)	(mbarn)	(mbarn)	(mbarn)		stat	sys[b]	tot
8	317.8±32.	1357.±12.	0.0	1675.	34.	12.	36.
10	211.9±21.	1244.±8.9	0.0	1456.	23.	11.	25.
15	99.6±10.	1039.±5.4	0.0	1139.	11.	9.4	14.
20	57.6±5.8	902.0±3.8	0.0	959.6	6.9	8.1	11.
25	37.5±3.8	802.9±3.0	0.3	840.7	4.8	7.2	8.7
30	26.3±2.6	726.5±2.5	1.0	753.8	3.6	6.5	7.4
40	15.0±1.5	613.0±1.9	5.1±0.1	633.1	2.4	5.6	6.1
50	9.7±1.0	529.2±1.6	12.7±0.4	551.6	1.9	4.9	5.3
52	9.0±0.9	514.8±1.6	14.6±0.4	538.4	1.9	4.8	5.2
60	6.8±0.7	462.7±1.4	22.8±0.7	492.3	1.7	4.4	4.7
70	5.0±0.5	407.9±1.2	33.7±1.1	446.6	1.7	4.0	4.3
80	3.8±0.4	361.9±1.1	44.3±1.5	410.0	1.9	3.7	4.2
90	3.0±0.3	322.9±1.0	54.0±1.9	379.9	2.2	3.4	4.0
100	2.5±0.3	289.5±0.9	62.6±2.3	354.6	2.5	3.2	4.1

Table 21 (continued)

^{174}Yb							
ΔE	0 - 3 keV	3 - 225 keV	225 - 700 keV	Thermal Spectrum			
Data:	see text	this work	from Ref. [10][a]				
kT	I_1	I_2	I_3	$<\sigma v>/v_T$ (mbarn)			
(keV)	(mbarn)	(mbarn)	(mbarn)		stat	sys[b]	tot
8	45.8±2.3	259.1±5.6	0.0	304.9	6.1	2.6	6.6
10	30.5±1.5	240.8±4.1	0.0	271.3	4.4	2.4	5.0
15	14.3±0.7	206.1±2.3	0.0	220.4	2.4	2.1	3.2
20	8.3±0.4	181.4±1.6	0.0	189.7	1.6	1.8	2.4
25	5.4±0.3	162.1±1.2	0.0	167.5	1.2	1.6	2.0
30	3.8±0.2	146.5±1.0	0.2	150.5	1.0	1.5	1.8
40	2.2±0.1	122.2±0.7	0.9	125.3	0.7	1.2	1.4
50	1.4±0.1	104.1±0.6	2.3±0.1	107.8	0.6	1.0	1.2
52	1.3±0.1	101.0±0.5	2.7±0.1	105.0	0.5	1.0	1.1
60	1.0±0.1	89.8±0.5	4.3±0.1	95.1	0.5	0.9	1.0
70	0.7±0.0	78.3±0.4	6.4±0.2	85.4	0.4	0.8	0.9
80	0.5±0.0	68.9±0.4	8.6±0.3	78.0	0.5	0.8	0.9
90	0.4±0.0	61.0±0.3	10.7±0.4	72.1	0.5	0.7	0.9
100	0.4±0.0	54.3±0.3	12.6±0.5	67.3	0.6	0.7	0.9
^{176}Yb							
ΔE	0 - 3 keV	3 - 225 keV	225 - 700 keV	Thermal Spectrum			
Data:	see text	this work	from Ref. [10][a]				
kT	I_1	I_2	I_3	$<\sigma v>/v_T$ (mbarn)			
(keV)	(mbarn)	(mbarn)	(mbarn)		stat	sys[b]	tot
8	40.9±2.0	199.7±5.7	0.0	240.6	6.0	3.2	6.8
10	27.3±1.4	185.9±4.2	0.0	213.2	4.4	3.0	5.3
15	12.8±0.6	159.0±2.4	0.0	171.8	2.5	2.5	3.5
20	7.4±0.4	139.6±1.6	0.0	147.0	1.6	2.2	2.7
25	4.8±0.2	124.6±1.2	0.0	129.4	1.2	2.0	2.3
30	3.4±0.2	112.4±0.9	0.1	115.9	0.9	1.8	2.0
40	1.9±0.1	93.5±0.7	0.6	96.0	0.7	1.5	1.7
50	1.2±0.1	79.3±0.5	1.6	82.1	0.5	1.3	1.4
52	1.2±0.1	76.9±0.5	1.8±0.1	79.9	0.5	1.3	1.4
60	0.9±0.0	68.2±0.5	2.9±0.1	72.0	0.5	1.1	1.2
70	0.6±0.0	59.3±0.4	4.3±0.1	64.2	0.4	1.0	1.1
80	0.5±0.0	52.0±0.3	5.8±0.2	58.3	0.4	0.9	1.0
90	0.4±0.0	45.9±0.3	7.2±0.3	53.5	0.4	0.8	0.9
100	0.3±0.0	40.8±0.3	8.5±0.3	49.6	0.4	0.8	0.9

[a]Normalized to present data

[b]The 1.5% uncertainty of the gold standard is not included here, since it cancels out in most applications of relevance for nuclear astrophysics

Table 22: MAXWELLIAN AVERAGED CROSS SECTIONS AT kT=30 keV COMPARED TO PREVIOUS EXPERIMENTS AND EVALUATIONS

Isotope	Experiment		Evaluation	
	Cross section (mb)	Reference	Bao and Käppeler [29]	Beer, Voss, Winters [30]
^{170}Yb	768.3 ± 7.2	present work[a]	727±29	738±29
	713 ± 28	Beer *et al.* (81)[b] [11]		
	731 ± 29	Beer *et al.* (84)[b] [12]		
	739 ± 56	Allen and Cohen (79)[b] [13]		
	989 ± 50	Bokhovko *et al.* (91) [10]		
^{171}Yb	1210. ± 12.	present work[a]	1411±51	1411±51
	1397 ± 50	Beer *et al.* (84)[b] [12]		
	1347 ± 111	Shorin *et al.* (75)[b] [9]		
	1371 ± 69	Bokhovko *et al.* (91)[10]		
^{172}Yb	341.3 ± 3.0	present work[a]	410 ±34	410 ±34
	400±33	Shorin *et al.* (75)[b] [9]		
	420 ± 25	Bokhovko *et al.* (91)[10]		
^{173}Yb	753.8 ± 7.4	present work[a]	865±72	865 ± 72
	802 ± 67	Shorin *et al.* (75)[b] [9]		
	868 ± 43	Bokhovko *et al.* (91) [10]		
^{174}Yb	150.5 ± 1.8	present work[a]	176 ± 16	176 ± 16
	163 ±15	Shorin *et al.* (75)[b] [9]		
	173 ± 14	Bokhovko *et al.* (91) [10]		
^{176}Yb	115.9± 2.0	present work[a]	111 ± 11	
	103 ±10	Shorin *et al.* (75)[b] [9]		
	136 ±11	Bokhovko *et al.* (91)[10]		
	208 ±40	Stupegia *et al.* (68)[14]		

[a] The 1.5% uncertainty of the gold cross section is not included, since it cancels out in most applications of relevance for nuclear astrophysics.
[b] These data have been normalized to compensate for different gold cross sections [31].

References

[1] K. Wisshak, K. Guber, F. Voss, F. Käppeler, and G. Reffo, Phys. Rev. C **48**, 1401 (1993).

[2] K. Wisshak, F. Voss, F. Käppeler, K. Guber, L. Kazakov, N. Kornilov, M. Uhl, and G. Reffo, Phys. Rev. C. **52**, 2762 (1995).

[3] K. Wisshak, F. Voss, F. Käppeler, L. Kazakov, and G. Reffo, Phys. Rev. C. **57**, 391 (1998).

[4] F. Voss, K. Wisshak, K. Käppeler, and L. Kazakov, Report FZKA 6104, Forschungszentrum Karlsruhe, Karlsruhe, Germany 1998.

[5] E. Anders and N. Grevesse, Geochim. Cosmochim. Acta **53**, 197 (1989).

[6] F. Käppeler, Proc. of the 2nd Oak Ridge Symposium on Atomic and Nuclear Astrophysics, 2–6 Dec. 1997. IOP Publishing Bristol and Philadelphia 1998.

[7] O. Straniero, R. Gallino, M. Busso, A. Chieffi, C.M. Raiteri, M. Limongi, and M. Salaris, Astrophys. J. **440**, L85 (1995).

[8] R. Gallino, C. Arlandini, M. Busso, M. Lugaro, C. Travaglio, O. Straniero, A. Chieffi, and M. Limongi, Astrophys. J. **497**, 388 (1998).

[9] V.S. Shorin, V.N. Kononov, and E.D. Poletaev, Sov. J. Nucl. Phys. **20**, 572 (1975).

[10] M.V. Bokhovko, V.N. Kononov, E.D. Poletaev, N.S. Rabotnov, and V.M. Timokhov, Proc. Int. Conf. on Nuclear Data for Science and Technology, Jülich, Germany, 1991 (Springer Berlin, Heidelberg, New York 1992) p.62.

[11] H. Beer, F. Käppeler, K. Wisshak, and R.A. Ward, Astrophys. J. Suppl. **46**, 295 (1981).

[12] H. Beer, G. Walter, R.L. Macklin, and P.J. Patchett, Phys. Rev. C **30**, 464 (1984).

[13] B.J. Allen and D.D. Cohen, Aust. J. Phys., **32**, 447 (1979).

[14] D.C. Stupegia, C.R. Keedy, M. Schmidt, A.A. Madson, J. Nucl. Energy, **22**, 267 (1968).

[15] K. Wisshak, F. Voss, F. Käppeler, and G. Reffo, Phys. Rev. C **45**, 2470 (1992).

[16] K. Wisshak, K. Guber, F. Käppeler, J. Krisch, H. Müller, G. Rupp, and F. Voss, Nucl. Instr. Meth. A **292**, 595 (1990).

[17] K. Wisshak, F. Voss, F. Käppeler, and G. Reffo, Phys. Rev. C **42**, 1731 (1990).

[18] F. H. Fröhner, Technical report, Gulf General Atomic (unpublished).

[19] C. Nordborg, H. Gruppelaar, and M. Salvatores, in *Nuclear Data for Science and Technology*, edited by S. Qaim (Springer, Berlin, 1992), p. 782.

[20] V. McLane, C.L. Dunford, and P.F. Rose, in *Neutron Cross Sections, Vol. 2,* (Academic Press, New York, 1988).

[21] K. Wisshak, F. Voss, F. Käppeler, L. Kazakov, and G. Reffo, Report FZKA 5967, Forschungszentrum Karlsruhe, Karlsruhe, Germany 1997.

[22] A. Gilbert and A.G.W. Cameron, Can. J. Phys. **43**, 1446 (1965).

[23] J. F. Mughabghab, M. Divadeenam, and N. E. Holden, in *Neutron Cross Sections, Vol. 1, Part A* (Academic Press, New York, 1981).

[24] F. Voss, K. Wisshak, K. Guber, F.Käppeler, and G. Reffo, Phys. Rev. C **50**, 2582 (1994).

[25] R. L. Macklin, private communication (unpublished).

[26] W. Ratynski and F. Käppeler, Phys. Rev. C **37**, 595 (1988).

[27] J. Kopecky, J.-Ch. Sublet, J.A. Simpson, R.A. Forrest, and D. Nierop, Report INDC(NDS)-362, International Atomic Energy Agency, Vienna, Austria, 1997.

[28] K. Wisshak, F. Voss, and F. Käppeler, Report FZKA–5968, Forschungszentrum Karlsruhe, 1997.

[29] Z. Y. Bao and F. Käppeler, Atomic Data Nucl. Data Tables **36**, 411 (1987).

[30] H. Beer, F. Voss, and R.R. Winters, Astrophys. J. Suppl. **80**, 403 (1992).

[31] Z. Y. Bao, private communications 1995.